Tetrahedron 64 (2008) 10837–10848

Contents lists available at ScienceDirect

Tetrahedron

journal homepage: www.elsevier.com/locate/tet

DNMR, DFT and preparative study on the conformation of (*Z*)-4,5,6,7-tetrahydropyrazolo[1,5-*e*]benzo[*g*][1,5]diazonin-8-ones and (*Z*)-4,5-dihydropyrazolo[1,5-*d*]benzo[*f*][1,4]diazocin-7(6*H*)-ones

Ádám Gyömöre [a], Zoltán Kovács [a], Tibor Nagy [b], Veronika Kudar [c], András Szabó [d], Antal Csámpai [a,*]

[a] *Institute of Chemistry, Eötvös Loránd University, PO Box 32, H-1518 Budapest-112, Hungary*
[b] *Research Group for Protein Modelling, Hungarian Academy of Sciences, Eötvös Loránd University, PO Box 32, H-1518 Budapest-112, Hungary*
[c] *Chemres Institute of Structural Chemistry Chemical Research Center, Hungarian Academy of Sciences, PO Box 17, H-1518 Budapest, Hungary*
[d] *Ubichem Research Ltd, PO Box 17, H-1518 Budapest, Hungary*

ARTICLE INFO

Article history:
Received 16 June 2008
Received in revised form 19 August 2008
Accepted 4 September 2008
Available online 17 September 2008

Keywords:
Benzodiazonine
Benzodiazocine
Ring inversion
Conformational flexibility
DNMR
DFT

ABSTRACT

By means of base-catalyzed ring enlargement of triazaindenoindenes and pentalenoindenes obtained from anhydride-induced ring transformation of 3,4-dihydro-2*H*-pyrimido- and 2,3-dihydroimidazo[2,1-*a*]phthalazinium-olates, respectively, a series of pyrazolo[1,5-*e*]benzo[*g*][1,5]diazonin-8-ones and pyrazolo[1,5-*d*]benzo[*f*][1,4]diazocin-7(6*H*)-ones were obtained. Alternative pathways and energetics for the ring inversion of symmetrically substituted medium-size ring systems were determined by combined use of DNMR measurements and B3LYP/6-31G(d,p) calculations using the IEFPCM solvent model. One pyrazolobenzodiazonine carrying hydrogen at the C1 position was found to undergo facile ring inversion by a two-step mechanism, while 1-Me and 1-Ph substituents rendered complete rigidity to this ring system. A three-step mechanism was revealed for the ring inversion of the two studied pyrazolobenzodiazocines with energetics practically invariant to the investigated *C*1-substituents (H and Me). The attempted RCM of the *N*,*O*-diallyl derivative of a selected rigid model effected by Grubbs II catalyst led to deallylation and olefin isomerization avoiding the formation of bridged products with enhanced skeletal strain. A tolerable degree of ring strain associated with negligible skeletal distortion could be introduced into the same benzodiazonine by N,O-dialkylation with 1,3-bis(bromomethyl)benzene.

1. Introduction

Medium ring heterocycles are often encountered in biologically active natural products as well as drug candidates. However, medium-sized rings are difficult to prepare due to enthalpic and entropic reasons, and direct cyclization methods are ineffective unless certain conformational restraints are present in the acyclic precursor.[1] Interesting structures containing medium-size heterorings with valuable biological effects have also been obtained by a variety of ring transformation reactions.[2–11] Bicyclic benzo[*g*][1,5]diazonines obtained by base-mediated ring enlargement of aryl-*N*-methylpyrazolo[1,2-*b*]phthalazinium iodides[2a] have been shown to display pronounced CNS-activity.[2b] Different benzodiazocines and benzodiazonines are preferably obtained from oxidative ring expansion of polycyclic fused compounds often containing indole unit[3–5] or intramolecular transacylation of 1-[2-(ω-aminoalkyl)-phenyl]azetidin-2-ones.[6] On the other hand, the primary formation of medium-size rings can be immediately followed by a variety of trans-annular interactions leading to ring contraction. For instance, alternative trans-annular condensations of 3,4,5,6-tetrahydro-1*H*-benzo[*e*][1,4]diazonine-2,7-diones transitionally formed by the oxidative ring fission of 1,2,3,4-tetrahydrocarbolines led to the formation of 1,2,3,4-tetrahydropyrrolo[3,4-*b*]quinolinones[7a] or 1,2,3,4-tetrahydropyrrolo [2,3-*c*]quinolinones.[7b] Another example is the ring isomerization of pyridazino[1,2-*c*][1,3,4]thiadiazinones into thiazolo[3,4-*a*][1,3]diazepinones proceeding by the cleavage of the N–N bond followed by trans-annular recyclization of the intermediate 1,3,8-thiadiazecinones.[8] In biological fluids the biological activity of medium-size heterocycles depends not only on pharmacophoric grouping,[9] but also on the conformation.[10] By means of combined use of NMR, X-ray analysis and molecular modelling, the structural and energetic aspects of the ring inversion of some benzodiazepine and benzotriazepine derivatives were studied in detail establishing nonplanar, rapidly interconverting (on the NMR time scale) boat shape conformation for the seven membered ring in agreement with the results of X-ray analyses.[9–15]

* Corresponding author. Tel.: +36 01 209 0555; fax: +36 01 372 2909.
E-mail address: csampai@chem.elte.hu (A. Csámpai).

0040-4020/$ – see front matter © 2008 Elsevier Ltd. All rights reserved.
doi:10.1016/j.tet.2008.09.020

Experimental and theoretical conformational studies of the more flexible benzodiazocine and benzodiazonines have also been reported,[5,16–20] but there are a relatively low number of examples of synthesis and structural analysis of their polycyclic hetero-condensed derivatives.[21–27] To our knowledge no theoretical modelling even on tricyclic benzodiazocines and benzodiazonines exists. These facts impelled us to initiate comparative preparative, DNMR and theoretical study on the conformation of pyrazolobenzodiazonines **5a**,**b**[27] and **5c** (Scheme 1) and related diazocines **9e**–**i** (Scheme 2). The preparation of **5c** and **9e**–**i** is also described in this paper.

2. Results and discussion

2.1. Preparation of model compounds

In 1988 Körmendy et al. observed that, on treatment with aqueous $NaHCO_3$ at reflux temperature, tetracyclic triazaindenoindenes **2a**,**b** underwent trans-annular ring opening via deacylated intermediates **4a**,**b** affording **5a**,**b** in maximum yields ca. 50%.[27] This limited yield was attributed to competitive hydrolytic fission of the *N*-acylated pyrazole ring leading to carboxylic acids **3a**,**b** (Scheme 1) and other undefined products.[27] Avoiding the undesirable conversions we selectively accomplished the deacylation of N3 pyrazole nitrogen with hydrazinehydrate in refluxing ethanol and obtained **4a**,**b** in 80–88% yield. (Deacetylation leading to **4a** in a maximum of 51% yield has been achieved by heating **2a** for ca. 10 min in aqueous $NaHCO_3$.[28]) Ring enlargement of **4a** and **4b** effected by aqueous $NaHCO_3$ took place almost quantitatively (92% and 96%, respectively) via the assumed '*E*'-lactams **IVa**,**b**. The treatment of **5a**,**b** with boiling acetic anhydride (Scheme 1) afforded **6a**,**b** with aromatic pyrazole ring[27] without reconstruction of tetracyclic system type **2**. We found that pyrazolobenzodiazonines **5a**,**b** can easily be recovered by hydrazinolysis of **6a**,**b** taking place without the cleavage of the nine-membered lactam ring.

Since **2a**,**b**, the potential precursors of medium-size ring systems, were prepared by ring transformation of pyrimido[2,1-*a*]phthalazinium-olate **1** taking place with the incorporation of RCH–CO motif of the anhydride component,[28] we tried to employ phenylacetic anhydride as reagent to extend the group of model compounds with a phenyl-substituted analogue. When the reaction was conducted at 140 °C, zwitterion **1** was directly transformed into *N*,*O*-diacylated 1-phenylpyrazolo[1,5-*d*]benzodiazonine **6c** (Scheme 1). The facile conversion of triazaindenoindene **2c**, the assumed intermediate, is suggested to start with equilibrium trans-annular ring enlargement to **Ic** retaining the lactam motif with '*E*' configuration, which is preformed in **2c**. The propensity of **2c** to undergo trans-annular ring opening can be ascribed to the enhanced steric repulsion between the 1-phenyl substituent and the condensed benzene ring, which interaction is decreased in **Ic**. Following equilibrium rotation about the N6a–C7 bond and N→O acyl migration (**Ic**→**IIc**→**IIIc**), the resulted '*Z*'-lactam **IIIc** is supposed to undergo N-acylation yielding **6c**, facile hydrazinolysis of which afforded **5c**. Diacyl derivatives **6a**,**b** were analyzed by ^{1}H, ^{13}C and ^{15}N NMR spectroscopy of which results were unambiguously confirmed by single crystal X-ray diffraction providing indirect evidence for the skeletal structure of the studied models **5a**–**c** (discussed later).

The view about the size-dependent effect of the group R on the propensity of triazaindenoendene skeleton to undergo isomerization into the corresponding pyrazolobenzodiazonine was supported by monitoring thermal conversions **4a**,**b**→**5a**,**b** by ^{1}H NMR spectroscopy in DMSO-d_6 solution. The reaction of **4b** could be completed at 340 K in 1 h, while **4a** proved to be stable at this temperature. On heating its solution at 370 K, ca. 40% conversion of **4a** could be achieved in 30 min. In order to get comparable theoretical results DFT calculations[29] were also carried out for relevant models (**4a**–**c** and **5a**–**c**) at B3LYP level of theory[30] using 6-31G(d,p) basis set [31] and IEFPCM solvent model,[32] which adequately represents the experimental conditions (solvent: DMSO, ε=46.70). The free energy differences for the overall conversions

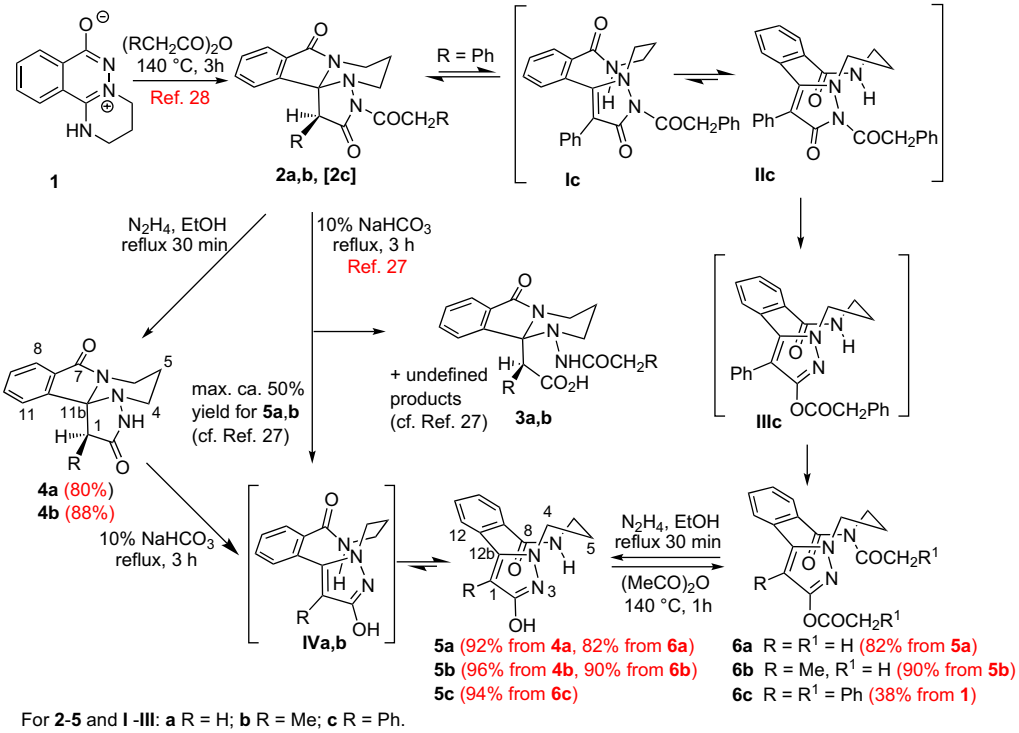

Scheme 1. Synthetic routes to model pyrazolobenzodiazonines **5a**–**c**.

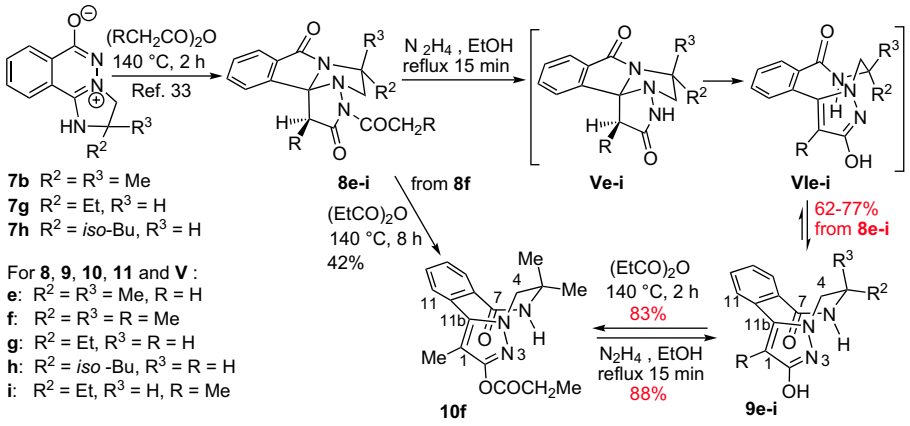

Scheme 2. Synthetic routes to model pyrazolobenzodiazocines **9e**–**i**.

4a–**c**→**5a**–**c** obtained after geometry optimization and subsequent frequency calculation show the expected R-group-dependence with the pronounced effect of the phenyl substituent [ΔG(**5**–**4**)=−0.59 kcal/mol for **a**; −1.95 kcal/mol for **b**; −6.23 kcal/mol for **c**]. Experimentally observable overall reactions (**4**→**IV**→**5**) are related to the analogue unobservable process (**2c**→**Ic**→**IIc**→**IIIc**), since both types of isomerizations presumably proceed via the corresponding '*E*'-lactam formed directly from the tetracyclic precursor.

In order to elaborate an expedient route to an analogous novel tricyclic ring system with eight-membered heterocycle we envisioned the two-step protocol involving hydrazine-mediated deacylation followed by base-catalyzed ring enlargement to the transformation of triazapentalenoindenes **8e**–**i**[33] into the corresponding pyrazolobenzodiazocine of type **9** (Scheme 2). The synthesis of **8e**–**i** was performed by the anhydride-induced ring transformation of zwitterionic 2,3-dihydroimidazo[2,1-*a*]phthalazinium-olates **7b**,**g**,**h** with sterically hindered N1 atom and sterically accessible N5 atom of which primary acylation is the prerequisite of the ring transformation of type **7**→**8**.[33] (This is the circumstance, which prevents the formation of simpler pyrazolobenzodiazocine models unsubstituted on position 5.)

To our surprise the hydrazinolysis of **8e**–**i** directly afforded **9e**–**i** in short time (15 min) with acceptable yields (62–77%) suggesting that the primarily formed deacetylated intermediates **Ve**–**i** undergo fast isomerization probably proceeding through *trans* lactams **VIe**–**i**. In keeping with this observation, B3LYP/6-31G(d,p)/IEFPCM calculations (ε=46.70) revealed that even isomerization **VIe**→**9e** (R=H) is approximately as exothermic as that of the ring opening postulated for its 1-phenyl-substituted ring homologue (**4c**→**5c**), which was discussed above [ΔG(**9e**–**Ve**)=−6.56 kcal/mol, ΔG(**5c**-**4c**)=−6.23 kcal/mol]. The enhanced tendency of tetracycles **Ve**–**i** to undergo ring opening can be attributed to the strain resulted from the annulation of three five-membered rings and to the repulsive interaction of the *endo*-oriented R^2 group and H1 atom being in steric proximity.[33] Indicating an additional destabilizing effect exerted by the Me1-group on the tetracyclic system, a more significant decrease in the free energy was calculated by the same method for the trans-annular ring opening of the assumed intermediate **Vf** [ΔG(**9f**–**Vf**)=−11.07 kcal/mol]. Accordingly, on prolonged treatment with propinic anhydride, **8f** underwent partial isomerization affording monopropionyl compound **10f** in moderate yield (42%). Demonstrating the steric hindrance of the N6 atom due to the adjacent methyl groups in a control experiment, on heating with propionic anhydride **9f** underwent acylation exclusively on the hydroxypyrazole unit to give **10f**. The propionyl group can be removed by facile hydrazinolysis without fission of the eight-membered lactam (**10f**→**9f**). It must be pointed out here that the eight-membered '*E*'-lactams **VIe**,**f** are also assumed to be involved as intermediates in the ring inversion of **9e**,**f** associated with racemization (discussed later).

2.2. Structural analysis of pyrazolobenzodiazonines and benzodiazocines

The ^{1}H, ^{13}C and ^{15}N NMR spectroscopic data measured in $CDCl_3$ at 300 K for diacyl derivatives **6a**,**b** are consistent with their solid state structures determined by X-ray diffraction (Figs. 1 and 2). The same skeletal structure was established for **6c** on the basis of ^{1}H, ^{13}C and ^{15}N NMR spectroscopic data, which are closely related to those of **6a**,**b**.

In **5a**–**c** and **6a**–**c** the chair-like fraction of the nine-membered ring composed by N3a, C4, C5, C6 and N7 is unambiguously reflected from the relatively large values (10–12 Hz) of vicinal coupling constants $^3J(H4_{ax},5H_{ax})$, $^3J(H5_{ax},6H_{ax})$ and $^3J(7NH_{ax},6H_{ax})$ showing approximately *anti*-periplanar position for the relevant atom pairs. The presence of this structural element was also supported by mutual NOEs (6–8%) detected between $H4_{ax}$ and $H6_{ax}$. The ^{1}H, ^{13}C and ^{15}N NMR parameters measured for **5a**–**c** in DMSO-d_6 at 300 K indicate basically the same structural characteristics with aromatic pyrazole ring. In the ^{1}H–^{15}N HMBC spectra the ^{15}N

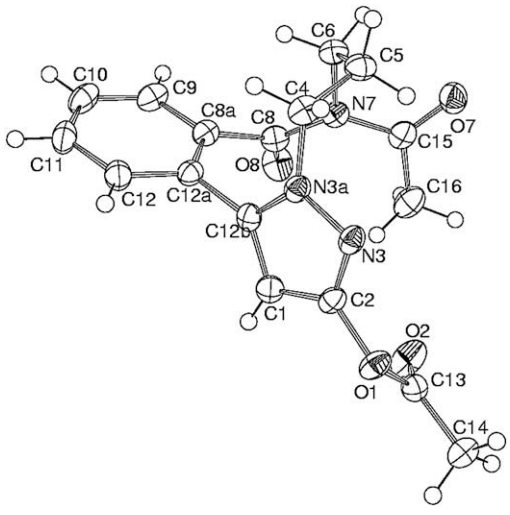

Figure 1. ORTEP structure of **6a**.

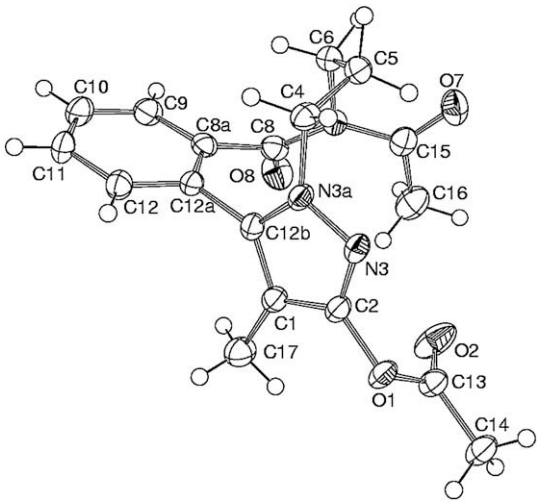

Figure 2. ORTEP structure of **6b**.

signals of N3 and N3a atoms can be identified from the intense cross-peaks with $H4_{ax}$ and $H5_{eq}$ signals, respectively, showing nearly *anti*-periplanar position of the strongly coupled nuclei. The downfielded N3 and N3a shifts measured for **5a–c** and **6a–c** [266–288 ppm for N3 and 180–184 ppm for N3a (relative to the signal of liquid NH_3)] indicate the aromatic character of the pyrazole ring, while the upfield shift of the same signals obtained for **4a**,**b** (159–162 ppm for N3 and 98–103 ppm for N3a) points to the presence of saturated pyrazolidine ring incorporating CONH motif. The dominance of this tautomer was unequivocally evidenced by the one-bond coupling between N3 and H3 nuclei via their satellite cross-peaks ($^1J_{N-H}$=95 Hz) detected in the $^1H-^{15}N$ HMBC spectra. The lactam-acylation in **6a–c** is spectacularly reflected from the significantly downfield-shifted N7 resonance (172 ppm for each). The analogous signals of **5a–c** were detected at 122–124 ppm.

In **9e–i** the presence of an aromatic hydroxypyrazole ring and the '*Z*'-lactam is evidenced by the related ^1H, ^{13}C and ^{15}N NMR data, which are very similar to those obtained for the analogous benzodiazonine derivatives (see Section 4). Considerable NOEs (9–11%) were measured between the NH and the protons of the R^2 group pointing to their relative cis position on the *exo* side of the eight-membered ring. Since the R^2 group is *endo*-situated in tetracycles of type **8**,[33] this configuration gives indirect support for the assumed mechanism of the two-step conversion of unisolable tetracycles **Ve–i** proceeding through **VIe–i** containing R^2 and the pyrazole ring in cis position relative to each other. As additional support for the boat conformation of the eight-membered ring, in **9e**,**f** mutual NOEs (3–5%) were detected between the protons of the *endo*-positioned methyl group (R^3=Me) and the H8 proton of the condensed benzene ring.

2.3. Ring inversion

The conformational flexibility of the model pyrazolobenzodiazonines **5a–c** and selected pyrazolobenzodiazocines **9e**,**f** with symmetric substitution pattern was investigated by DNMR measurements and DFT analysis of the potential energy surface. The calculations were carried out at B3LYP/6-31G(d,p) level of theory using IEFPCM solvent model (solvent: DMSO, ε=46.70). Ring inversion associated with racemization was monitored by ^1H NMR spectroscopy employing DMSO-d_6 as solvent. The separated signals of diastereotopic skeletal protons completely coalesced at 333 K for **5a**. By heating the solutions of **5b** and **5c** up to 370 K no coalescence could be detected, even line broadening was not observable on the separated signals, showing that the bulky *C*1-substituents on the pyrazole moiety highly enhance the rigidity of the whole skeleton. In contrast to the studied nine-membered ring system, pyrazolobenzodiazocines **9e**,**f** exhibited only a practically negligible substituent-dependence in the conformational flexibility characterized by very similar coalescence temperatures (355 K for **9e** and 360 K for **9f**). The Eyring equation[34] using the coalescence temperature and chemical shift difference of the most separated signal pairs of geminal ring protons [$\Delta\nu(H4_{ax}-H4_{eq})$=300 Hz for **5a–c** and 140 Hz for **9e**,**f**] afforded 15.8 kcal/mol for **5a**, 17.9 kcal/mol for **9e** and 18.2 kcal/mol for **9f** as experimental activation free energy ($\Delta G^{\ddagger}_{exp}$, Table 1). In the absence of coalescence temperature no $\Delta G^{\ddagger}_{exp}$ could be obtained for **5b** and **5c**.

Theoretical modeling of the investigated ring inversions was applied to reveal the mechanisms. One-step racemization of **5a–c** and **9e**,**f** would proceed via transition states with internal mirror plane, which are associated with fully planar ring systems. Since such structures could not be located on the potential energy surface (PES) by none of the applied methods (Berny analytical gradient optimization,[35] QST2 and QST3 analyses[36]), one-step inversion can be ruled out as a possible mechanism for each investigated model. Two further pathways involving two and three steps, respectively (A and B), were taken into consideration and studied in detail (Schemes 3 and 4). [The (+) and (−) signs are arbitrary representations of the enantiomeric forms.] The stationary points were characterized by frequency calculations in order to verify that minima and transition structures have zero and one imaginary frequency, respectively.[37] The ring inversion along path A involves two separate flips of the lactam and the condensed pyrazole motifs sweeping through the plane of the benzene ring. Single local minimum containing oppositely oriented lactam and pyrazole motifs (**VIIa**, Scheme 3) could be localized exclusively for the racemization of benzodiazonine **5a**. In the first transition state (**TS1/A/5a**) the lactam unit and the benzene ring and in the second transition state (**TS2/A/5a**) the benzene and the pyrazole rings are nearly coplanar (interplanar angles Θ=4.4° and 0.1°, respectively). (The calculated **TS** structures are collected on Fig. 3.) With bulky R-substituents neither analogous saddle point structures (**TS2/A/5b**,**c**) nor local minimum structures (**VIIb**,**c**) could be located on the PESs, indicating that pathway A can be ruled out as a possible ring inversion mechanism for the rigid benzodiazonines **5b**,**c**. This mechanism must again be discarded for the ring inversion of benzodiazocine models **9e**,**f** as structures **IXe**,**f** (Scheme 4) could not be located as local minima on

Table 1
Measured coalescence temperatures (T_{coal} [K]) and experimental activation free energy values ($\Delta G^{\ddagger}_{exp}$ [kcal/mol])[a] for the alternative ring inversions (paths A and B) of **5a–c** and **10e**,**f**, and theoretical activation free energy values ($\Delta G^{\ddagger}_{\pm n}$ [kcal/mol])[b] for the possible elementary steps (cf. Schemes 3 and 4, respectively)

Inv. of	T_{coal} [K]	$\Delta G^{\ddagger}_{exp}$	$\Delta G^{\ddagger}_1$/A	$\Delta G^{\ddagger}_2$/A	$\Delta G^{\ddagger}_1$/B	$\Delta G^{\ddagger}_2$/B	$\Delta G^{\ddagger}_3$/B
			$\Delta G^{\ddagger}_{-1}$/A	$\Delta G^{\ddagger}_{-2}$/A	$\Delta G^{\ddagger}_{-1}$/B	$\Delta G^{\ddagger}_{-2}$/B	$\Delta G^{\ddagger}_{-3}$/B
5a	333	15.8	13.3	2.2	19.7	21.8	17.9
			2.5	13.1	14.3	20.3	24.8
5b	—[c]	—	—		18.8	24.6	17.9
					10.7	24.9	25.6
5c	—[c]	—	—	—	18.9	25.1	18.0
					12.0	26.0	24.0
10e	355	17.9	—	—	14.6	17.1	10.3
					6.9	14.6	20.5
10f	360	18.2	—	—	16.5	17.9	10.5
					6.3	17.3	21.3

[a] Obtained by Eyring equation using the T_{coal} and $\Delta\nu$ values extracted from DNMR measurements, which were carried out in DMSO-d_6 solution.
[b] Obtained by B3LYP/6-31G(d,p) level of DFT calculations using IEFPCM solvent model (DMSO, ε=46.70) representing the experimental conditions.
[c] No coalescence could be observed. For technical precaution the temperature was not raised above 370 K, which was obviously far from the coalescence conditions.

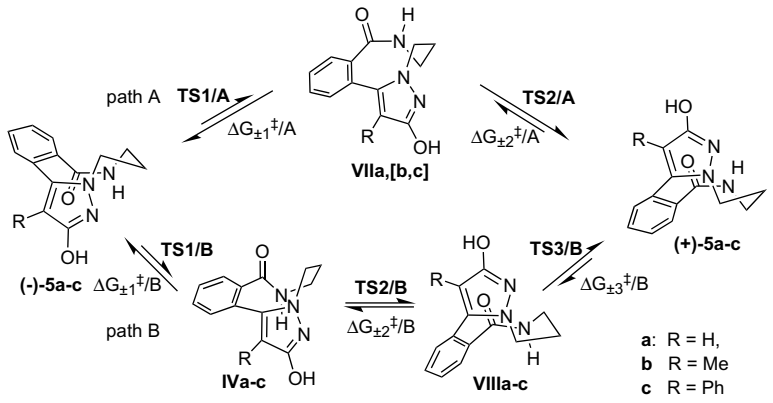

Scheme 3. Ring inversion pathways of model pyrazolobenzodiazonines **5a**–**c**.

the PESs. When started from input structures of type **IX** having oppositely oriented 'Z'-lactam and pyrazole units, geometry optimizations ended up in global minima **9e**,**f**. (Similarly, when started from input structures generated from the real local minimum **VIIa** by replacing H1 for Me and Ph groups, respectively, geometry optimizations resulted in global minima **5b**,**c**.)

Pathway B comprising three separate steps with two local minima and three transition states could be traced and analyzed for the racemization of each studied model compound. The first step is the $Z \rightarrow E$ isomerization of the lactam unit by the rotation of the oxo group taking place through the *exo* side of the ring systems [(−)-**5a**–**c**→**IVa**–**c**: Scheme 3; (−)-**9e**,**f**→**VIe**,**f**: Scheme 4]. In the subsequent steps the flip of the pyrazole ring [**IVa**–**c**→**VIIIa**–**c**: Scheme 3; **VIe**,**f**→**Xe**,**f**: Scheme 4] is followed by the $E \rightarrow Z$ isomerization of the lactam unit taking place with the rotation of the NH group [**VIIIa**–**c**→(+)-**5a**–**c**: Scheme 3; **Xe**,**f**→(+)-**9e**,**f**: Scheme 4]. The TS structures collected in Figure 3 (**TS1/A**, **TS2/A** for **5a** and **TS1/3/B** for each model) were obtained as QST3/B3LYP/6-31G(d,p)/IEFPCM refinements of input structures resulted from QST2 calculations carried out at HF/6-31G level of ab initio theory. The final results of DFT calculations (Table 1) show that in the course of racemization of **5a**–**c** proceeding along path B the flip of the pyrazole ring has the highest barrier with transition state of type **TS2/B**, which must be destabilized by the repulsion between the *C*1-substituent and H12 situated close to each other. Due to steric crowding associated with the presence of bulky *C*1-methyl and phenyl substituents, **TS2/B/5b** and **TS2/B/5c** represent very high barriers to this step ($\Delta G_2^{\ddagger}$/B=24.6 kcal/mol for **5b** and 25.1 kcal/mol for **5c**: Table 1), which could be overcome at around 500 K. These calculated values are in accord with the experimentally observed extreme rigidity of **5b**,**c**. Since **TS2/B/5a** representing a high barrier ($\Delta G_2^{\ddagger}$/B=21.8 kcal/mol, Table 1), which could be passed at around 450 K, path B cannot be taken into account for the observed facile racemization of **5a**. The energetics calculated for path A fit much better to the experimental activation free energy of the racemization of **5a** (Table 1) and suggest that the order of elementary steps might be reversed as the two transition states are of similar in energy. On the other hand, the activation free energies calculated for the racemization of **9e**,**f** along path B (Table 1) show that the order of elementary steps cannot be reversed because lactam isomerization step **9**→**X** (Scheme 4) is prevented by high barrier ($\Delta G_{-3}^{\ddagger}$/B=20.5 kcal/mol for **9e** and 21.3 kcal/mol for **9f**), which could be passed at around 440–450 K. On the other hand, suggesting that the ring inversion of **9e**,**f** proceeds along path B, the experimental energetic data match satisfactorily with the activation free energy values calculated for the flip of pyrazole ring, the rate-limiting second elementary step (Table 1). This step is associated with much lower barrier for the racemization of **9e**,**f** than calculated for that of **5a**–**c**. Due to the enhanced interatomic distance the repulsive interaction between H1 and H11 is significantly smaller in **TS2/B/9e** than the analogous interaction in **TS2/B/5a** involving H12 (d_{H1-H11}=2.262 Å in **TS2/B/9e**, d_{H1-H12}=1.926 Å in **TS2/B/5a**). This is the consequence of the different interplanar angles between the benzene and pyrazole motifs computed for **TS2/B/9e** (Θ=31.7°) and **TS2/B/5a** (Θ=16.9°), respectively. Accordingly, as reflected from the corresponding $\Delta G_2^{\ddagger}$/B values listed in Table 1, the degree of steric crowding is almost equivalent in **TS2/B/9e** and **TS2/B/9f**, while the replacement of H1 in **TS2/B/5a** for bulkier substituents significantly enhances the energy of TS structures **TS2/B/5b** and **TS2/B/5c**.

In summary, comparison of experimental and calculated activation free energy values leads to the conclusion that the

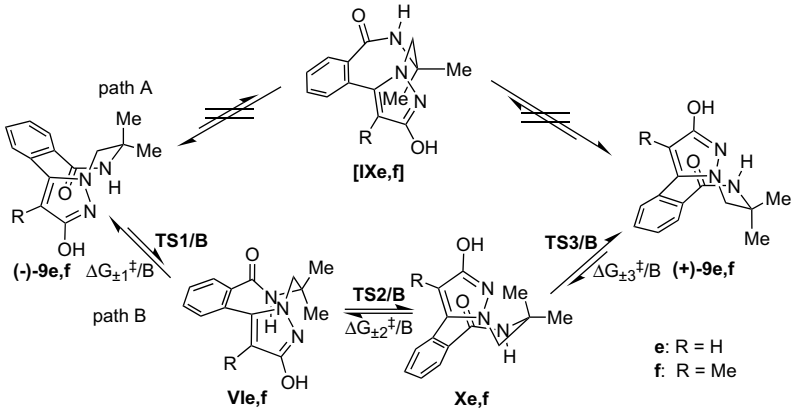

Scheme 4. Ring inversion pathways of model pyrazolobenzodiazocines **9e**,**f**.

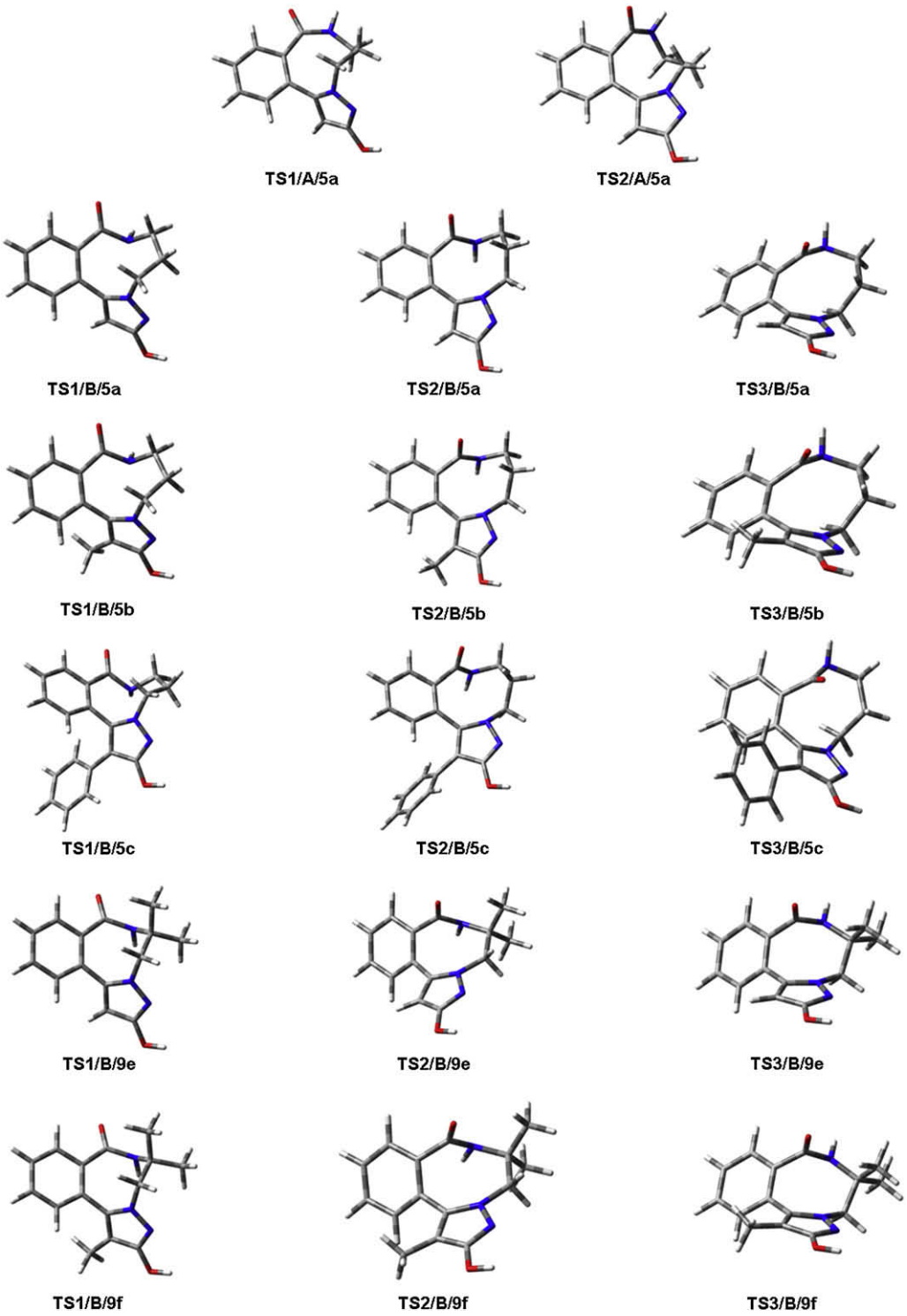

Figure 3. Transition state structures for the ring inversion of **5a–c** and **9e**,**f** calculated by B3LYP/6-31G(d,p)/IEFPCM (ε=46.70).

racemization of **5a** proceeds via path A, but the racemization of **5b**,**c** along this path is not an allowed process. The ring inversion of these rigid models was found to progress along path B, but could be effected only at highly elevated temperature because of the high barrier calculated for the second step. On the other hand, the racemization of **9e**,**f** is allowed to take place along path B with the rate determining flip of pyrazole ring, of which barrier is almost invariant to the size of the investigated R groups (H and Me).

2.4. Bridging reactions of the rigid pyrazolobenzo diazonine 5b

We wondered whether the conformationally rigid, readily available pyrazolobenzodiazonine **5b** with sterically accessible lactam NH group is capable of undergoing such bridging reactions, which are accompanied by more or less skeletal distortion, so we attempted its overbridging by olefin ring closing metathesis (RCM) and dialkylation protocols, respectively.

2.4.1. Allylation and attempted RCM reaction

First, diallylation of **5b** was performed in refluxing THF in the presence of NaH resulting in selectively *N*,*O*-diallyl derivative **11b** of which RCM[38] was attempted by 20 mol % of second generation Grubbs catalyst in benzene at reflux temperature (Scheme 5). Instead of the formation of bridged compounds (**XIb** and **XIIb**), N7-deallylation[39] and two types of olefin isomerization[40] took place as evidenced by the structures of isolated products **12b**, **13b** and **14b**. A synchronous 1,3-O→N-allyl migration must also be postulated for the formation of **14b** of which structure is evidenced by the following spectroscopic data: (i) appearance of the two amide-I bands in the IR spectrum (1662 and 1651 cm^{-1}); (ii) the C2 and C11b resonances are downfield-shifted (166.4 and 153.4 ppm, respectively) relative to those measured for **11b**–**13b** containing aromatic pyrazole ring (160.0–160.7 and 139.8–140.7 ppm, respectively); (iii) the N3 and N3a resonances are upfield-shifted (153 and 105 ppm, respectively) relative to those obtained for **11b**–**13b** (261–262 and 182 ppm, respectively).

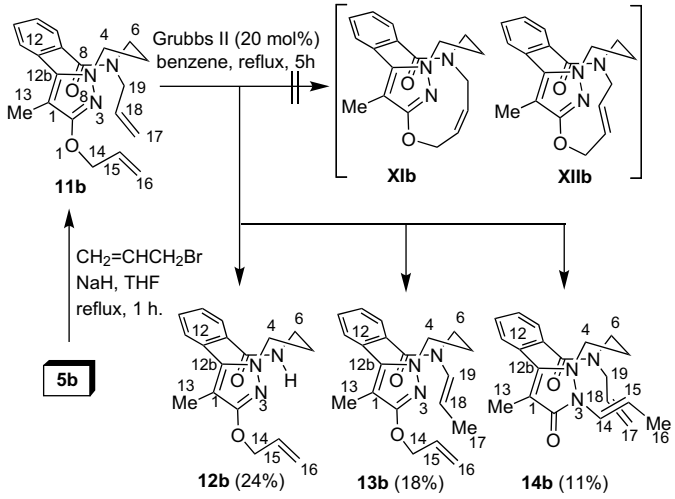

Scheme 5. Conversions of diallyl compound **11b** under the conditions of RCM.

The failure of RCM can be attributed to the high rigidity of the pyrazolobenzodiazonine skeleton inclined to avoid the considerable compression, which would be introduced by linking O1 and N7 atoms with the relatively short $CH_2CH{=}CHCH_2$ chain having either *Z* or *E* configuration. This assumption is in accord with the structural and thermochemical parameters calculated for **11b**, **XIb** and **XIIb** by B3LYP/6-31G(d,p) method. The overall skeletal compression is most spectacularly reflected from the change in the calculated O1–N7 distance, which is significantly shorter in **XIb** and **XIIb** than in **11b** (4.726 Å and 4.772 Å vs 5.465 Å). The changes in enthalpy for the hypothetical RCM reactions (ΔH=14.77 kcal/mol for **11b**→**XIb**+ethene and 10.55 kcal/mol for **11b**→**XIIb**+ethene) can be considered as good measure of the strain associated with the compression of the nine-membered ring. Since these processes are favoured from the aspect of entropy, the calculated changes in free energy are significantly smaller (6.73 kcal/mol and 4.77 kcal/mol, respectively).

2.4.2. Bridging by dialkylation

In order to check the possibility to introduce a minimal degree of strain into **5b** we also attempted its bridging with 1,3-bis(bromo methyl)benzene serving as a slightly more extended linker suitable to connect O1 and N7 atoms without significant distortion of the ring system. On treatment with this reagent and NaH in refluxing THF, **5b** partly underwent intramolecular dialkylation and the bridged product **15b** (Scheme 6) could be separated in 27% yield from the polymer-like substances formed in the reaction.

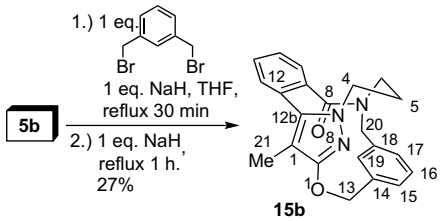

Scheme 6. Bridging of **5b** by dialkylation without introducing significant strain into the ring system.

The structure of **15b** was evidenced by single crystal X-ray analysis (Fig. 4) and also characterized by IR, ^1H, ^{13}C and ^{15}N NMR spectroscopy. The orientation of the bridging motif in $CDCl_3$ solution was proved by DNOE experiment disclosing interaction between the protons of Me21 group and H19 (5%). A small distortion was resulted from the bridging as reflected from the comparison of the O1–N7 distance measured for **15b** and the diacetyl derivative **6b** by X-ray analysis [5.345(2) Å and 5.260(2) Å, respectively, Table 2]. A smaller strain accumulated in **15b** than in **XIb** and **XIIb** as it can be estimated from the enthalpy change calculated by B3LYP/6-31G(d,p) method for the entropically favoured hypothetic reaction **5b**+1,3-bis(hydroxymethyl)-benzene→**15b**+$2H_2O$ involving covalent molecules (ΔH=6.74 kcal/mol, ΔG=0.28 kcal/mol).

*2.4.3. X-ray and DFT anylysis of **6a**,**b** and **15b***

It is worth pointing out that the bonding parameters obtained from X-ray diffraction and B3LYP/6-31G(d,p) optimization are in acceptable to good agreement (Table 2) indicating the sufficient reliability of the applied DFT method. In the experimental and the calculated structures of **6a**,**b** and **15b** the nine-membered ring adopts a bent conformation with eight atoms forming a boat shape (N3a, C4, C6, N7, C8, C8a, C12a and C12b) with the exception of C5 being on the tip (Figs. 1, 2 and 4). The planes of the pyrazole and benzene rings are nearly perpendicular to each other [X-ray/DFT interplanar angles defined by the torsion angle along the atomic sequence C8a–C12a–C12b–C1: 91.2(2)°/92.5° for **6a**, 87.9(2)°/88.9° for **6b** and 83.8(2)°/77.5° for **15b**]. The planes of the benzene ring and the carbonyl group of the *N*-substituted lactam moiety, defined by the torsion angle along the atomic sequence C12a–C8a–C8–O8, are not too far from being perpendicular (interplanar angles obtained X-ray/DFT: −113.9(2)°/−115.2° for **6a**, −118.2(2)°/−112.3° for **6b** and −101.6(2)°/−101.2° for **15b**).

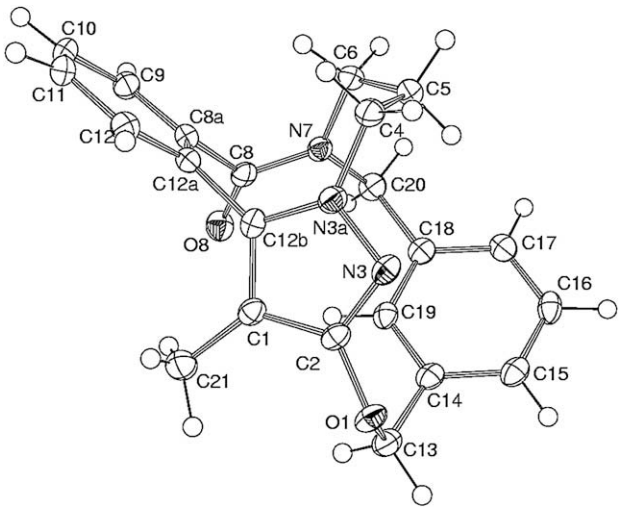

Figure 4. ORTEP structure of **15b**.

Table 2
Selected bonding parameters of **6a**,**b** and **15b** obtained by X-ray analysis and B3LYP/6-31G(d,p) calculations

	6a/X-ray	**6a**/DFT	**6b**/X-ray	**6b**/DFT	**15b**/X-ray	**15b**/DFT
Bond lengths [Å]						
C1–C2	1.391(2)	1.409	1.389(3)	1.413	1.408(2)	1.418
N3–C2	1.320(2)	1.328	1.326(2)	1.328	1.328(2)	1.325
N3–N3a	1.358(2)	1.355	1.360(2)	1.353	1.362(2)	1.361
N3a–C12b	1.356(2)	1.365	1.358(2)	1.367	1.359(2)	1.369
C1–C12b	1.377(2)	1.387	1.384(3)	1.391	1.382(2)	1.388
N3a–C4	1.456(2)	1.457	1.467(2)	1.457	1.455(2)	1.455
N7–C8	1.402(2)	1.405	1.401(2)	1.404	1.355(2)	1.375
Non-bonding distance [Å]						
O1···N7	5.295(2)		5.260(2)		5.345(2)	
Bond angles [°]						
N3–N3a–C12b	112.3(2)	112.5	112.2(2)	112.4	112.2(2)	111.9
N3–N3a–C4	118.4(2)	119.2	119.2(2)	119.4	119.1(2)	118.0
C4–N3a–C12b	128.9(2)	128.2	128.2(2)	127.9	127.4(2)	127.1
C6–N7–C8	115.8(2)	121.1	120.1(2)	121.4	124.4(2)	123.5
N7–C8–C8a	118.3(2)	117.8	117.4(2)	117.6	117.8(2)	118.3
Torsional angles [°]						
C8–C8a–C12a–C12b	−6.2(2)	−3.2	−2.2(3)	−2.6	−2.2(2)	−4.5
O8–C8–N7–C6	−148.4(2)	−151.0	−146.8(2)	−155.8	−171.8(2)	−170.2
C8a–C12a–C12b–C1	91.2(2)	92.5	87.9(2)	88.9	83.8(2)	77.5
C12a–C8a–C8–O8	−113.9(2)	−115.2	−118.2(2)	−112.3	−101.6(2)	−101.2

3. Conclusion

The facile formation of (*Z*)-4,5,6,7-tetrahydropyrazolo[1,5-*e*]benzo[*g*][1,5]diazonin-8-ones and (*Z*)-4,5-dihydropyrazolo[1,5-*d*]benzo[*f*][1,4]diazocin-7(6*H*)-ones by trans-annular ring enlargement of the appropriate fused tetracyclic compounds, their conformation as well as substituent- and ring-size-dependent molecular dynamics determined by the combined use of X-ray analysis, ^{1}H, ^{13}C, ^{15}N NMR, DNMR and DFT molecular modelling may contribute to understand the chemical reactivity and receptor-binding properties of medium-size angularly condensed heterocyclic compounds with potential biological interest. Since the experimental and theoretical energetic data discussed in this contribution are in good agreement and provide a possibility for decision between alternative mechanisms, it seems that standard B3LYP/6-31G(d,p) calculations employing polarizable continuum model are reasonable and reliable methods for studying ring inversion of related ring systems.

4. Experimental

4.1. General

All chemicals were obtained from commercially available sources and used without further purification (Aldrich, Fluka). Benzene and THF for the RCM and dialkylation reactions, respectively, were freshly distilled and dried by standard methods. All solvents for the crystallizations were used without additional purification. Each flash silica gel column chromatography was carried out on Merck Kieselgel 60 (230–400 mesh). Melting points were determined with a Boethius microstage and are uncorrected. The IR spectra were run in KBr disks on a Bruker IFS-55 FT-spectrometer controlled by Opus 3.0 software. The ^{1}H and ^{13}C NMR spectra were recorded in DMSO-d_6 or $CDCl_3$ solution in 5 mm tubes at rt, on a Bruker DRX-500 spectrometer at 500.13 (^{1}H), 125.76 (^{13}C) and 50.12 (^{15}N) MHz, with the deuterium signal of the solvent as the lock and TMS as internal standard (for ^{1}H and ^{13}C NMR) and NH_{3liq} as external reference (^{15}N NMR). The ^{15}N NMR chemical shifts were obtained and assigned from the 2D ^{1}H–^{15}N HMBC spectra. The standard Bruker microprogram NOEMULT to generate NOE and to get DIFFNOE spectra was used with a selective pre-irradiation time. DEPT spectra were run in a standard manner, using only Θ=135° pulse to separate the CH/CH_3 and CH_2 lines phased 'up' and 'down', respectively. The 2D-COSY, HMQC and HMBC spectra were obtained by using the standard Bruker pulse programs. All calculations were carried out with the Gaussian 03 suite of programs.[41] Optimized structures of all stationary points on PES's are available from the authors. All X-ray diffraction measurements were made on a Rigaku R-AXIS Rapid IP diffractometer at low temperatures using an X-Stream 2000 unit. Crystals were mounted in loops in high viscosity oil droplet. Crystal data were collected using standard X-scan procedures, with graphite monochromated Mo Kα radiation. Initial structure model obtained by direct methods (SHELXS97)[42] gave most of the non-hydrogen atoms, rest of which were subsequently located and refined to their final positions via full matrix least squares (SHELXL97)[43] following standard procedures. The hydrogen atoms were located from difference density maps and refined by riding model. All crystallographic data are deposited at the Cambridge Crystallographic Data Centre (deposit numbers: 687068 for **6a**; 687069 for **6b**; 687071 for **15b**) and can be obtained free of charge via www.ccdc.cam.ac.uk/data_request/cif, or by emailing data_request@ccdc.cam.ac.uk. Crystal data and refinement parameters are listed in a table in Supplementary data.

4.2. General procedure for the hydrazinolysis of tetracycles 2a,b, 8e–i and tricycles 6a–c and 10f

To a suspension of the corresponding precursor (1 mmol) in EtOH (10 mL) was added 92% $N_2H_4\cdot H_2O$ (100 μL dissolved in 1 mL of EtOH) dropwise under Ar atmosphere at rt, and the mixture was stirred and refluxed for 30 min (for **2a**,**b** and **6a**–**c**), or for 15 min (for **8e**–**i** and **10f**). The resulted yellow solution was cooled by ice-water, neutralized with a few drops of AcOH and after standing for ca. 30 min the precipitated crystals were filtered off and washed with a cooled 7:3 mixture of MeOH–water (5 mL). Analytical samples were obtained by recrystallization: EtOH (**4a**,**b**); DMF–EtOH (**5a**–**c** and **9e**–**i**). After filtration from DMF–EtOH, **5a**–**c** and **9e**–**i** were washed with EtOH and dried over P_2O_5 at 78 °C.

4.3. Data of triazaindeno[3,3a-*a*]indene-2(3*H*),7-diones, pyrazolobenzodiazonones and pyrazolobenzodiazocines

*4.3.1. 5,6-Dihydro-1H,4H,7H-3,3a,6a-triazaindeno[3,3a-a]indene-2(3H),7-dione (**4a**)*

Yield: white solid, 0.195 g, 80% (from **2a**); mp 174–175 °C (lit. [28] 173–174 °C); ν_{max} 3200, 1695, 1605 cm^{-1}; ^{1}H NMR (DMSO-d_6) δ 10.08 (1H, s, N*H*), 7.72 (1H, br d, *J*=7.3 Hz, H8), 7.64 (1H, td, *J*=7.3, 1.2 Hz, H9), 7.54–7.56 (overlapping, 2H, m, H10 and H11), 4.19 (1H, tdd, *J*=12.7, 4.4, 1.7 Hz, $H6_{eq}$), 3.62 (1H, d, *J*=16.6 Hz, $H1_{endo}$), 3.22 (1H, dt, *J*=11.3, 3.4 Hz, $H4_{eq}$), 3.15 (1H, td, *J*=12.7, 3.4 Hz, $H6_{ax}$), 2.92 (1H, td, *J*=11.5, 2.7 Hz, $H4_{ax}$), 2.18 (1H, d, *J*=16.6 Hz, $H1_{exo}$), 1.71 (1H, br d, *J*=12.7 Hz, $H5_{eq}$), 1.42 (1H, qa, *J*=12.7, 1.7 Hz, $H5_{ax}$); ^{13}C NMR (DMSO-d_6) δ 174.5 (C7), 167.0 (C2), 149.0 (C11a), 133.7 (C10), 130.5 (C9), 130.3 (C7a), 123.9 (C8), 122.1 (C11), 80.7 (C11b), 55.7 (C4), 35.9 (C6), 33.8 (C1), 24.5 (C5); ^{15}N NMR (DMSO-d_6) δ 162 (N3), 128 (N6a), 103 (N3a). Anal. Calcd for $C_{13}H_{13}N_3O_2$ (243.26): C, 64.19; H, 5.39; N, 17.27. Found: C, 64.25; H 5.35; N, 17.30%.

4.3.2. (1R,11bR*)-5,6-Dihydro-1-methyl-1H,4H,7H-3,3a,6a-triazaindeno[3,3a-a]indene-2(3H),7-dione (**4b**)*

Yield: white solid, 0.226 g, 88% (from **2b**); mp 184–186 °C; ν_{max} 3230, 1692, 1610 cm^{-1}; ^{1}H NMR (DMSO-d_6) δ 10.11 (1H, s, N*H*), 7.76 (1H, d, *J*=7.5 Hz, H8), 7.63 (1H, t, *J*=7.3 Hz, H10), 7.56 7.63 (1H, t, *J*=7.3 Hz, H9), 7.41 (1H, d, *J*=7.5 Hz, H11), 4.21 (1H, br d, *J*=12.8 Hz, $H6_{eq}$), 3.70 (1H, qa, *J*=7.1 Hz, H1), 3.20–3.16 (2H, m, $H4_{eq}$ and $H6_{ax}$), 3.07 (1H, t, *J*=11.3 Hz, $H4_{ax}$), 1.72 (1H, br d, *J*=13.2 Hz, $H5_{eq}$),

1.43 (1H, qa, J=13.1, 3.0 Hz, H5$_{ax}$), 0.56 (3H, d, J=7.1 Hz, 1-CH_3); ^{13}C NMR (DMSO-d_6) δ 176.3 (C7), 167.1 (C2), 145.5 (C11a), 133.0 (C10), 131.4 (C7a), 130.4 (C9), 124.3 (C8), 123.3 (C11), 84.5 (C11b), 54.7 (C4), 35.9 (C6), 34.8 (C1), 24.8 (C5), 8.9 (1-CH_3); ^{15}N NMR (DMSO-d_6) δ 159 (N3), 127 (N6a), 98 (N3a). Anal. Calcd for $C_{14}H_{15}N_3O_2$ (257.29): C, 65.35; H, 5.88; N, 16.33. Found: C, 65.30; H, 5.94; N, 16.40%.

4.3.3. (Z)-4,5,6,7-Tetrahydro-2-hydroxypyrazolo[1,5-e]benzo[g][1,5]diazonin-8-one (**5a**)

Yield: white solid, 0.199 g, 82% (from **6a**); mp 326–330 °C sublim. (lit.[27] >300 °C); ν_{max} 3200–2400 (br), 1669, 1615, 1550 cm^{-1}; ^{1}H NMR (DMSO-d_6) δ 9.58 (1H, s, O*H*), 7.67 (1H, t, J=7.2 Hz, N*H*), 7.54 (1H, td, J=7.3, 1.8 Hz, H10), 7.49 (1H, td, J=7.3, 1.8 Hz, H11), 7.35 (1H, dd, J=7.4, 2.0 Hz, H9), 7.33 (1H, dd, J=7.3, 1.8 Hz, H12), 5.37 (1H, s, H1), 3.92 (1H, br d, J=13.0 Hz, H4$_{eq}$), 3.49 (1H, br t, J=12.8 Hz, H4$_{ax}$), 3.17 (1H, br d, J=14.3 Hz, H6$_{eq}$), 2.79 (1H, m, H6$_{ax}$), 1.66 (1H, qa, J=13.7 Hz, H5$_{ax}$), 1.50 (1H, br d, J=13.7 Hz, H5$_{eq}$); ^{13}C NMR (DMSO-d_6) δ 171.1 (C8), 160.7 (C2), 141.4 (C12b), 140.3 (C8a), 130.5 (two coalesced lines, C10 and C12), 129.4 (C11), 128.9 (C12a), 126.3 (C9), 93.5 (C1), 50.7 (C4), 44.0 (C6), 31.0 (C5); ^{15}N NMR (DMSO-d_6) δ 268 (N3), 182 (N3a), 124 (N7). Anal. Calcd for $C_{13}H_{13}N_3O_2$ (243.26): C, 64.19; H, 5.39; N, 17.27. Found: C, 64.15; H 5.44; N, 17.32%.

4.3.4. (Z)-1-Methyl-4,5,6,7-tetrahydro-2-hydroxypyrazolo[1,5-e]benzo[g][1,5]diazonin-8-one (**5b**)

Yield: white solid, 0.232 g, 90% (from **6b**); mp 320–323 °C sublim. (lit.[27] >310 °C); ν_{max} 3295, 3180–2300 (br), 1662, 1625, 1568 cm^{-1}; ^{1}H NMR (DMSO-d_6) δ 9.44 (1H, s, O*H*), 7.61 (1H, dd, J=9.5, 4.9 Hz, N*H*), 7.54 (1H, td, J=7.3, 1.5 Hz, H10), 7.50 (1H, td, J=7.3, 1.5 Hz, H11), 7.35 (1H, dd, J=7.8, 1.5 Hz, H9), 7.30 (1H, dd, J=7.3, 1.5 Hz, H12), 3.88 (br d, J=13.9 Hz, H4$_{eq}$), 3.42 (1H, dd, J=13.9, 10.8 Hz, H4$_{ax}$), 3.14 (1H, dt, J=15.2, 4.9 Hz, H6$_{eq}$), 2.74 (1H, dt, J=15.2, 10.7 Hz, H6$_{ax}$), 1.63 (1H, qa, J=13.2 Hz, H5$_{ax}$), 1.50 (3H, s, 1-CH_3), 1.47 (1H, dt, J=13.2, 4.3 Hz, H5$_{eq}$); ^{13}C NMR (DMSO-d_6) δ 171.2 (C8), 159.2 (C2), 140.6 (C8a), 139.9 (C12b), 130.7 (C12), 130.4 (C10), 129.6 (C11), 128.6 (C12a), 126.4 (C9), 100.5 (C1), 50.7 (C4), 44.0 (C6), 31.6 (C5), 7.3 (1-CH_3); ^{15}N NMR (DMSO-d_6) δ 266 (N3), 180 (N3a), 124 (N7). Anal. Calcd for $C_{14}H_{15}N_3O_2$ (257.29): C, 65.35; H, 5.88; N, 16.33. Found: C, 65.41; H, 5.90; N, 16.41%.

4.3.5. (Z)-4,5,6,7-Tetrahydro-2-hydroxy-1-phenylpyrazolo[1,5-e]benzo[g][1,5]diazonin-8-one (**5c**)

Yield: white solid, 0.300 g, 94% (from **6c**); mp >360 °C; ν_{max} 3260–2300 (br), 1662, 1611, 1573, 1221, 1184, 764 cm^{-1}; ^{1}H NMR (DMSO-d_6) δ 10.11 (1H, s, O*H*), 7.83 (1H, dd, J=9.6, 4.9 Hz, N*H*), 7.58 (1H, td, J=7.7, 1.5 Hz, H10), 7.47 (1H, td, J=7.7, 1.5 Hz, H11), 7.43 (1H, br d, J=7.7 Hz, H9), 7.29 (1H, br d, J=7.5 Hz, H12), 7.19 (2H, dd, J=7.5, 1.3 Hz, H2′ of 1-Ph), 7.09 (2H, t, J=7.5 Hz, H3′ of 1-Ph), 7.00 (1H, tt, J=7.7, 1.3 Hz, H4′ of 1-Ph), 3.97 (1H, br d, J=14.9 Hz, H4$_{eq}$), 3.48 (1H, dd, J=14.9, 12.1 Hz, H4$_{ax}$), 3.22 (1H, dt, J=15.0, 4.6 Hz, H6$_{eq}$), 2.89 (1H, dt, J=15.0, 9.8 Hz, H6$_{ax}$), 1.77 (1H, br qa, J=13.0 Hz, H5$_{ax}$), 1.58 (1H, dt, J=14.5, 4.7 Hz, H5$_{eq}$); ^{13}C NMR (DMSO-d_6) δ 171.3 (C8), 158.4 (C2), 141.0 (C8a), 138.6 (C12b), 133.4 (C1′ of 1-Ph), 130.8 (two coalesced lines, C10 and C12), 129.8 (C11), 128.6 (C12a), 128.5 (C3′ of 1-Ph), 126.6 (C9), 125.7 (C4′ of 1-Ph), 106.0 (C1), 50.8 (C4), 44.0 (C6), 31.0 (C5); ^{15}N NMR (DMSO-d_6) δ 266 (N3), 188 (N3a), 122 (N7). Anal. Calcd for $C_{19}H_{17}N_3O_2$ (319.36): C, 71.46; H, 5.37; N, 13.16. Found: C, 71.42; H, 5.33; N, 13.21%.

4.3.6. (Z)-4,5-Dihydro-2-hydroxy-5,5-dimethylpyrazolo[1,5-d]benzo[f][1,4]diazocin-7(6H)-one (**9e**)

Yield: white solid, 0.196 g, 76% (from **8e**); mp >360 °C; ν_{max} 3150–2200 (br), 1674, 1635, 1549, 1208, 1188, 782 cm^{-1}; ^{1}H NMR (DMSO-d_6) δ 9.75 (1H, s, O*H*), 7.69 (1H, s, N*H*), 7.55–7.51 (overlapping, 3H, m, H8, H9 and H10), 7.23 (1H, m, H11), 5.70 (1H, s, H1), 3.79 (1H, d, J=15.4 Hz, H4$_{exo}$), 3.51 (1H, J=15.4 Hz, H4$_{endo}$), 1.30 (3H, s, 5-CH_{3endo}), 1.10 (3H, s, 5-CH_{3exo}); ^{13}C NMR (DMSO-d_6) δ 170.9 (C7), 161.4 (C2), 143.3 (C11b), 139.2 (C7a), 130.8, 130.0 (two coalesced lines), 129.6 (C8–11), 127.7 (C11a), 90.4 (C1), 56.1 (C4), 55.0 (C5), 29.8 (5-CH_{3endo}), 29.1 (5-CH_{3exo}); ^{15}N NMR (DMSO-d_6) δ 271 (N3), 185 (N3a), 137 (N6). Anal. Calcd for $C_{14}H_{15}N_3O_2$ (257.29): C, 65.35; H, 5.88; N, 16.33. Found: C, 65.37; H, 5.94; N, 16.29%.

4.3.7. (Z)-4,5-Dihydro-2-hydroxy-1,5,5-trimethylpyrazolo[1,5-d]benzo[f][1,4]diazocin-7(6H)-one (**9f**)

Yield: white solid, 0.193 g, 71% (from **8f**); 0.239 g, 88% (from **10f**); mp >360 °C; ν_{max} 3275, 3210–2350 (br), 1669, 1622, 1538, 1220, 1177, 790 cm^{-1}; ^{1}H NMR (DMSO-d_6) δ 9.67 (1H, s, O*H*), 7.56 (1H, s, N*H*), 7.58–7.53 (overlapping, 3H, m, H8, H9 and H10), 7.28 (1H, m, H11), 3.74 (1H, d, J=15.4 Hz, H4$_{exo}$), 3.50 (1H, J=15.4 Hz, H4$_{endo}$), 1.83 (3H, s, 1-CH_3), 1.34 (3H, s, 5-CH_{3endo}), 1.12 (3H, s, 5-CH_{3exo}); ^{13}C NMR (DMSO-d_6) δ 170.9 (C7), 160.0 (C2), 140.3 (C7a), 139.8 (C11b), 130.6, 130.01, 129.99, 129.7 (C8–11), 127.5 (C11a), 97.7 (C1), 56.1 (C4), 55.0 (C5), 29.6 (5-CH_{3endo}), 29.2 (5-CH_{3exo}); ^{15}N NMR (DMSO-d_6) δ 270 (N3), 184 (N3a), 137 (N6). Anal. Calcd for $C_{15}H_{17}N_3O_2$ (271.31): C, 66.40; H, 6.32; N, 15.49. Found: C, 66.44; H, 6.39; N, 15.47%.

4.3.8. (Z)-(exo)-5-Ethyl-4,5-dihydo-2-hydroxypyrazolo[1,5-d]benzo[f][1,4]diazocin-7(6H)-one (**9g**)

Yield: white solid, 0.160 g, 62% (from **8g**); mp 300–304 °C; ν_{max} 3305, 3130–2300 (br), 1675, 1610, 1531, 1212, 1191, 800 cm^{-1}; ^{1}H NMR (DMSO-d_6) δ 9.26 (1H, s, O*H*), 8.06 (1H, d, J=9.4 Hz, N*H*), 7.48–7.44 (overlapping, 2H, m, H9 and H10), 7.36–7.32 (overlapping, 2H, m, H8 and H11), 5.50 (1H, s, H1), 3.97 (1H, dd, J=12.6, 3.0 Hz, 4H$_{endo}$), 3.78 (1H, t, J=12.6, 4H$_{exo}$), 3.44 (1H, m, 5H), 1.43 (2H, qui, J=7.0 Hz, CH_2CH$_3$), 0.78 (3H, t, J=7.0 Hz, CH$_2$CH_3); ^{13}C NMR (DMSO-d_6) δ 171.7 (C7), 161.2 (C2), 142.7 (C11b), 136.2 (C7a), 130.6 and 130.5 (C9 and C10), 130.1 (C8), 129.1 (C11a), 128.0 (C8), 95.8 (C1), 58.1 (C4), 53.3 (C5), 25.8 (CH_2CH$_3$), 11.4 (CH$_2$CH_3); ^{15}N NMR (DMSO-d_6) δ 272 (N3), 183 (N3a), 128 (N6). Anal. Calcd for $C_{14}H_{15}N_3O_2$ (257.29): C, 65.35; H, 5.88; N, 16.33. Found: C, 65.40; H, 5.90; N, 16.24%.

4.3.9. (Z)-(exo)-5-iso-Butyl-4,5-dihydro-2-hydroxypyrazolo[1,5-d]benzo[f][1,4]diazocin-7(6H)-one (**9h**)

Yield: white solid, 0.194 g, 68% (from **8h**); mp 285–287 °C; ν_{max} 3300, 3200–2300 (br), 1668, 1625, 1538, 1232, 1178, 776 cm^{-1}; ^{1}H NMR (DMSO-d_6) δ 9.25 (1H, br s, O*H*), 8.08 (1H, d, J=9.6 Hz, N*H*), 7.49–7.45 (overlapping, 2H, m, H9 and H10), 7.37–7.33 (overlapping, 2H, m, H8 and H11), 5.53 (1H, s, H1), 3.93 (1H, dd, J=13.5, 4.5 Hz, H4$_{endo}$), 3.79 (1H, t, J=13.5 Hz, H4$_{exo}$), 3.58 (1H, m, H5), 1.64 [1H, m, CH$_2$CH(CH$_3$)$_2$], 1.46 [1H, ddd, J=14.5, 11.3, 4.7 Hz, CH(H)CH(CH$_3$)$_2$], 1.09 [1H, ddd, J=14.5, 10.3, 3.4 Hz, CH(H)CH(CH$_3$)$_2$], 0.79 [3H, d, J=6.7 Hz, CH$_2$CH(CH_3)(CH$_3$)], 0.55 [3H, d, J=6.7 Hz, CH$_2$CH(CH$_3$)(CH_3)]; ^{13}C NMR (DMSO-d_6) δ 171.4 (C7), 161.0 (C2), 142.9 (C11b), 136.1 (C7a), 130.7 and 130.5 (C9 and C10), 130.1 (C8), 129.1 (C11a), 127.8 (C8), 95.7 (C1), 58.4 (C4), 49.6 (C5), 40.9 [CH$_2$CH(CH$_3$)$_2$], 24.8 [CH$_2$CH(CH$_3$)$_2$], 23.8 [CH$_2$CH(CH_3)(CH$_3$)], 21.5 [CH$_2$CH(CH$_3$)(CH_3)]; ^{15}N NMR (DMSO-d_6) δ 272 (N3), 185 (N3a), 129 (N6). Anal. Calcd for $C_{16}H_{19}N_3O_2$ (285.34): C, 67.35; H, 6.71; N, 14.73. Found: C, 67.28; H, 6.65; N, 14.74%.

4.3.10. (Z)-(exo)-5-Ethyl-4,5-dihydro-2-hydroxy-1-methylpyrazolo[1,5-d]benzo[f][1,4]diazocin-7(6H)-one (**9i**)

Yield: white solid, 0.209 g, 77% (from **8i**); mp 312–315 °C; ν_{max} 3295, 3180–2300 (br), 1662, 1625, 1545, 1210, 1158, 754 cm^{-1}; ^{1}H NMR (DMSO-d_6) δ 9.57 (1H, br s, O*H*), 7.96 (1H, d, J=9.4 Hz, N*H*), 7.49 (1H, t, J=7.3 Hz, H10), 7.45 (1H, t, J=7.3 Hz, H9), 7.34 (1H, d, J=7.3 Hz, H8), 7.27 (1H, d, J=7.3 Hz, H11), 3.92 (1H, dd, J=13.0, 5.0 Hz, H4$_{endo}$), 3.43 (1H, t, J=13.0 Hz, H4$_{exo}$), 3.37 (1H, m, H5), 1.62

(3H, s, 1-CH_3), 1.42 (2H, qui, J=7.0 Hz, CH_2CH$_3$), 0.78 (3H, t, J=7.0 Hz, CH$_2$CH_3); ^{13}C NMR (DMSO-d_6) δ 171.9 (C7), 159.8 (C2), 139.1 (C11b), 137.2 (C7a), 130.8 (C10), 130.2 (C9), 129.9 (C8), 129.6 (C11a), 127.9 (C11), 101.6 (C1), 57.8 (C4), 53.6 (C5), 25.2 (*C*H$_2$CH$_3$), 11.5 (CH$_2$*C*H$_3$), 7.9 (1-*C*H$_3$); ^{15}N NMR (DMSO-d_6) δ 270 (N3), 182 (N3a), 131 (N6). Anal. Calcd for $C_{15}H_{17}N_3O_2$ (271.31): C, 66.40; H, 6.32; N, 15.49. Found: C, 66.33; H, 6.37; N, 15.44%.

4.4. General procedure for base-catalyzed ring enlargement reactions 4a,b→5a,b

The mixture of the appropriate precursor (1 mmol) and 10% $NaHCO_3$ (10 mL) was refluxed for 3 h. The resulted yellow solution was cooled and its pH was adjusted to 5–6 by concd HCl. After standing for 1 h in refrigerator the precipitated crystals were collected, washed with water and dried. Yield: 0.224 g, 92% for **5a**; 0.247 g, 96% for **5b**. Analytical samples were obtained by recrystallization from EtOH. Within experimental error spectroscopic and analytical data proved to be identical with those listed in Sections 4.3.3 and 4.3.4, respectively.

4.5. General procedure for anhydride-induced transformations of 5a,b, 8f and 9f

A mixture of the corresponding precursor (1 mmol) and anhydride (50 mmol) was heated at 140 °C for the following periods of time: 1 h (**5a**,**b**+acetic anhydride); 8 h (**8f**+propionic anhydride); 2 h (**9f**+propionic anhydride). The excess of the acetic or propionic anhydride was distilled under reduced pressure (2–5 mBa; the temperature of oil bath was kept at 90–110 °C). The resulted brownish solid was triturated with methanol, filtered off, thoroughly washed with water and extracted with DCM (30 mL). The solution was dried over $MgSO_4$ and evaporated to dryness. The residue was subjected to column flash chromatography using *n*-hexane–EtOAc (5:1) as eluent yielding **6a**,**b** or the unreacted **8f**. The undissolved monopropionyl compound **10f** (from **8f** and **9f**) contaminated by some tarry substances was purified by flash column chromatography using DCM–MeOH (20:1) as eluent. Analytical samples were recrystallized: **6a**,**b** (DCM–cyclohexane); **10f** (EtOH).

4.6. Data of the acylated medium-size heterocycles

*4.6.1. (Z)-7-Acetyl-2-acetoxy-4,5,6,7-tetrahydropyrazolo[1,5-e]benzo[g][1,5]diazonin-8-one (**6a**)*

Yield: white prisms, 0.268 g, 82% (from **5a**); mp 153–155 °C (lit.[27] 154–155 °C); ν_{max} 1754, 1690, 1568, 1548, 1212, 1178, 772 cm^{-1}; ^{1}H NMR (CDCl$_3$) δ 7.64–7.56 (overlapping, m, 3H, H9–11), 7.43 (1H, m, H12), 6.13 (1H, s, H1), 4.17 (1H, br d, J=15.3 Hz, H4$_{eq}$) 4.09 (1H, dd, J=15.0, 4.5 Hz, H6$_{eq}$), 3.85 (1H, br t, J=14.1 Hz, H4$_{ax}$), 3.01 (1H, dd, J=14.5, 11.4 Hz, H6$_{ax}$), 2.29 (3H, s, OCOCH_3), 2.23 (3H, s, NCOCH_3) overlapping with 2.21 (1H, br qa, J=14.9 Hz, H5$_{ax}$), 1.60 (1H, br d, J=15.0 Hz, H5$_{eq}$); ^{13}C NMR (CDCl$_3$) δ 172.9 (N*C*OCH$_3$), 172.7 (C8), 167.5 (O*C*OCH$_3$), 154.3 (C2), 140.3 (C8a), 138.7 (C12b), 130.5 (C10), 130.4 (C11), 130.0 (C9), 127.2 (two coalesced lines, C12 and C12a), 98.5 (C1), 49.9 (C4), 46.0 (C6), 27.1 (C5), 26.1 (NCO*C*H$_3$), 20.7 (OCO*C*H$_3$); ^{15}N NMR (CDCl$_3$) δ 278 (N3), 194 (N3a), 172 (N7). Anal. Calcd for $C_{17}H_{17}N_3O_4$ (327.33): C, 62.38; H, 5.23; N, 12.84. Found: C, 62.33; H, 5.26; N, 12.88%.

*4.6.2. (Z)-7-Acetyl-2-acetoxy-4,5,6,7-tetrahydro-1-methylpyrazolo[1,5-e]benzo[g][1,5]diazonin-8-one (**6b**)*

Yield: white plates, 0.307 g, 90% (from **5b**); mp 179–181 °C; ν_{max} 1771, 1683, 1567, 1513, 1224, 1172, 769 cm^{-1}; ^{1}H NMR (CDCl$_3$) δ 7.66–7.61 (overlapping m, 2H, H10 and H11), 7.58 (1H, m, H9), 7.43 (1H, m, H12), 4.16 (1H, br d, J=15.1 Hz, H4$_{eq}$) slightly overlapping with 4.11 (1H, dd, J=15.1, 4.7 Hz, H6$_{eq}$), 3.76 (1H, ddd, J=15.1, 12.7, 1.7 Hz, H4$_{ax}$), 3.01 (1H, dd, J=14.7, 11.8 Hz, H6$_{ax}$), 2.30 (3H, s, OCOCH_3), 2.23 (3H, s, NCOCH_3) overlapping with 2.22 (1H, br qa, J=14.9 Hz, H5$_{ax}$), 1.66 (3H, s, 1-CH_3), 1.54 (1H, br d, J=15.1 Hz, H5$_{eq}$); ^{13}C NMR (CDCl$_3$) δ 173.6 (N*C*OCH$_3$), 173.3 (C8), 168.6 (O*C*OCH$_3$), 153.6 (C2), 139.4 (C8a), 139.2 (C12b), 131.12 and 131.07 (C10 and C11), 130.7 (C9), 127.6 (C12), 127.1 (C12a), 107.5 (C1), 50.1 (C4), 46.3 (C6), 27.3 (C5), 26.2 (NCO*C*H$_3$), 20.9 (OCO*C*H$_3$), 7.0 (1-*C*H$_3$); ^{15}N NMR (CDCl$_3$) δ 279 (N3), 193 (N3a), 172 (N7). Anal. Calcd for $C_{18}H_{19}N_3O_4$ (341.36): C, 63.33; H, 5.61; N, 12.31. Found: C, 63.40; H, 5.57; N, 12.28%.

*4.6.3. (Z)-4,5-Dihydro-1-methyl-2-propionyloxypyrazolo[1,5-d]benzo[f][1,4]diazocin-7(6H)-one (**10f**)*

Yield: pale yellow solid, 0.137 g, 42% (from **8f**) and 0.272 g, 83% (from **9f**); mp 215–217 °C; ν_{max} 3305, 1765, 1641, 1583, 1551, 1222, 1154, 744 cm^{-1}; ^{1}H NMR (CDCl$_3$) δ 7.69 (1H, m, H8), 7.57–7.51 (overlapping, m, 2H, H9–10), 7.31 (1H, m, H11), 5.77 (1H, s, N*H*), 3.93 (1H, d, J=15.1 Hz, H4$_{exo}$), 3.83 (1H, d, J=15.1 Hz, H4$_{endo}$), 2.64 (2H, qa, J=7.6 Hz, OCOCH_2CH$_3$), 1.89 (3H, s, 1-CH_3), 1.47 (3H, s, 5-CH_{3endo}), 1.29 (3H, t, J=7.6 Hz, OCOCH$_2$CH_3), 1.26 (3H, s, 5-CH_{3exo}), ^{13}C NMR (CDCl$_3$) δ 172.5 (O*C*OCH$_2$CH$_3$), 171.6 (C7), 154.1 (C2), 141.0 (C11b), 138.0 (C7a), 131.0 (C10), 130.3 (C9), 130.1 (C8), 130.0 (C11), 127.1 (C11a), 105.1 (C1), 56.4 (C4), 55.5 (C5), 30.1 (5-*C*H$_{3endo}$), 29.5 (5-*C*H$_{3exo}$), 27.7 (OCO*C*H$_2$CH$_3$), 9.5 (OCOCH$_2$*C*H$_3$), 7.5 (1-*C*H$_3$). Anal. Calcd for $C_{18}H_{21}N_3O_3$ (327.38): C, 66.04; H, 6.47; N, 12.84. Found: C, 65.99; H, 6.50; N, 12.80%.

4.7. (*Z*)-4,5,6,7-Tetrahydro-1-phenyl-7-phenacetyl-2-phenacetoxypyrazolo[1,5-*e*]benzo[*g*][1,5]diazonin-8-one (6c)

The mixture of **1a** (2.01 g, 10 mmol) and phenylacetic anhydride (12.70 g, 50 mmol) was kept at 140 °C for 3 h. To the cooled brownish mixture ethanol (40 mL) was added and the resulted solution was stirred for 2 h at rt and kept overnight in refrigerator. The precipitated colourless microcrystals were filtered off, washed with cold EtOH (5 mL) and dried. Analytical sample was recrystallized from DCM–cyclohexane. Yield: white small needles, 0.211 g, 38% (from **1a**); mp 203–205 °C; ν_{max} 1761, 1689, 1578, 1525, 1220, 1164, 753 cm^{-1}; ^{1}H NMR (CDCl$_3$) δ 7.60–7.53 (overlapping, 3H, m, H9–11), 7.43 (1H, d, J=7.3 Hz, H12), 7.30–7.18 (overlapping, 10H, m, OCOCH$_2$*Ph* and NCOCH$_2$*Ph*), 7.08–7.00 (overlapping, 3H, m, H3′–5′ of 1-Ph), 6.94 (2H, d, J=7.7 Hz, H2′ of 1-Ph), 4.24 (1H, br d, J=12.0 Hz, H4$_{eq}$), 4.17 (1H, br d, J=12.8 Hz, H6$_{eq}$), 4.06 (1H, d, J=16.7 Hz, NCOC*H*HC$_6$H$_5$), 3.83–3.77 (overlapping, m, 3H, H4$_{ax}$ and OCOCH_2C$_6$H$_5$), 3.60 (1H, d, J=16.7 Hz, NCOCH*H*C$_6$H$_5$), 3.08 (1H, t, J=12.8 Hz, H6$_{ax}$), 2.31 (1H, br qa, J=15.3 Hz, H5$_{ax}$), 1.55 (1H, br d, J=15.3 Hz, H5$_{eq}$); ^{13}C NMR (CDCl$_3$) δ 175.0 (C8), 169.2 (O*C*OCH$_2$Ph), 152.4 (C2), 139.7 (C8a), 138.5 (C12b), 135.2 (C1′ of NCOCH$_2$Ph), 133.2 (C1′ of OCOCH$_2$Ph), 130.1 (C1′ of 1-Ph), 131.33, 131.29, 131.25, 130.3, 129.9, 129.1, 128.9, 128.6 (two coalesced lines), 127.9 (two coalesced lines), 127.2, 127.1 (Ar–*C*H signals), 50.5 (C4), 46.7 (C6), 44.5 (NCO*C*H$_2$Ph), 41.5 (OCO*C*H$_2$Ph), 27.1 (C5); ^{15}N NMR (CDCl$_3$) δ 281 (N3), 196 (N3a), 172 (N7). Anal. Calcd for $C_{35}H_{29}N_3O_4$ (555.62): C, 75.66; H, 5.26; N, 7.56. Found: C, 75.59; H, 5.28; N, 7.60%.

4.8. N,O-Diallylation of 5b: preparation of (*Z*)-7-allyl-2-allyloxy-1-methyl-4,5,6,7-tetrahydropyrazolo[1,5-*e*]benzo[*g*][1,5]diazonin-8-one (11b)

Under Ar atmosphere to the mixture of NaH (0.48 g, 20 mmol) and THF (50 mL), **5b** (2.57 g, 10 mmol) was added in small portions. The resulted yellowish suspension was stirred for ca. 5–10 min at 25 °C until the hydrogen evolution was stopped. After dropwise addition of allylbromide (2.42 g, 20 mmol) the reaction mixture was refluxed for 1 h and evaporated to dryness. The oily residue

was dissolved in DCM (50 mL) and the undissolved salt was removed by filtration. The solution was extracted with water (2×50 mL), dried over $MgSO_4$ and evaporated. The oily residue was subjected to flash column chromatography using *n*-hexane–EtOAc (8:1) as eluent. The first band visible on UV-irradiation was collected and evaporated. On standing overnight under *n*-hexane in refrigerator the resulted pale yellow oil was solidified, filtered off and dried to obtain **11b** in analytically pure form. Yield: pale yellow microcrystals, 2.292 g, 68%; mp 131–133 °C; ν_{max} 1643, 1498, 1464, 1216, 1191, 786 cm^{-1}; ^1H NMR ($CDCl_3$) δ 7.52 (1H, td, J=7.7, 1.3 Hz, H10), 7.48 (1H, td, J=7.7, 1.3 Hz, H11), 7.44 (1H, dd, J=7.7, 1.3 Hz, H9), 7.32 (1H, br d, J=7.5 Hz, H12), 6.11 (1H, ddt, J=17.3, 10.6, 5.3 Hz, H15), 5.62 (1H, ddt, J=16.9, 10.8, 5.5 Hz, H18), 5.42 (1H, dqa, J=17.3, 1.7 Hz, $H16_{trans}$), 5.26 (1H, dqa, J=10.7, 1.7 Hz, $H16_{cis}$), 5.14 (1H, dqa, J=17.0, 1.5 Hz, $H17_{trans}$), 5.08 (1H, dqa, J=10.8, 1.5 Hz, $H17_{cis}$), 4.72 (2H, br d, J=5.3 Hz, H14), 4.11 (1H, dt, J=15.0, 3.2 Hz, $H4_{eq}$), 4.03 (1H, br dd, J=15.0, 5.3 Hz, $H6_{eq}$), 3.69 (1H, dd, J=15.0, 7.0 Hz, $H6_{ax}$), 3.62 (1H, ddd, J=15.0, 12.6, 2.1 Hz, $H4_{ax}$), 3.25 (2H, br d, J=5.5 Hz, H19), 2.15 (1H, m, $H5_{ax}$), 1.42 (1H, br d, J=15.2 Hz, $H5_{eq}$), 1.72 (3H, s, H13); ^{13}C NMR ($CDCl_3$) δ 170.0 (C8), 160.7 (C2), 140.7 (C12a), 140.2 (C8a), 134.2 (C15), 133.7 (C18), 130.5 (C11), 130.3 (C10), 129.3 (C9), 128.5 (C12a), 126.1 (C12), 117.8 (C16), 117.4 (C17), 102.5 (C1), 69.7 (C14), 50.3 (C4), 49.4 (C19), 48.1 (C6), 27.8 (C5), 6.6 (C13); ^{15}N NMR ($CDCl_3$) δ 261 (N3), 182 (N3a), 125 (N7). Anal. Calcd for $C_{20}H_{23}N_3O_2$ (337.42): C, 71.19; H, 6.87; N, 12.45. Found: C, 71.28; H, 6.88; N, 12.38%.

4.9. Attempted RCM of 11b

To the solution of **11b** (0.337 g, 1 mmol) in dry benzene (50 mL) previously degassed by Ar, $[Cl_2RuP(C_6H_{11})_3(=CHC_6H_5)$(1,3-dimesitylimidazol-2-ylene)] (0.187 g, 0.2 mmol) was added. The solution was stirred, refluxed for 5 h under Ar and evaporated to dryness. The resulted deep red mixture was subjected to flash column chromatography using *n*-hexane–EtOAc (4:1) as eluent. The first eluting band was put aside and the second well-separated fraction was collected, evaporated and the solid residue was recrystallized from EtOH to obtain **12b** in analytically pure form. The first band containing the mixture of **13b** and **14b** was separated as first and second bands, respectively, by repeated flash column chromatography using *n*-hexane–Et_2O (15:1) as eluent. On standing overnight under *n*-hexane in refrigerator, **13b** and **14b** were solidified, filtered off and dried to obtain analytically pure samples.

4.10. Data of the products obtained by attempted RCM of 11b

*4.10.1. (Z)-2-Allyloxy-1-methyl-4,5,6,7-tetrahydropyrazolo[1,5-e]benzo[g][1,5]diazonin-8-one (**12b**)*

Yield: pale yellow needles, 0.072 g, 24%; mp 254–256 °C; ν_{max} 3240, 1655, 1494, 1476, 1211, 1189, 780 cm^{-1}; ^1H NMR (DMSO-d_6) δ 7.51 (1H, t, J=7.7 Hz, H11), 7.47 (1H, t, J=7.7 Hz, H10), 7.43 (1H, br d, J=7.5 Hz, H9), 7.30 (1H, d, J=7.7 Hz, H12), 6.52 (1H, dd, J=9.1, 4.9 Hz, N*H*), 6.06 (1H, ddt, J=17.0, 10.5, 5.4 Hz, H15), 5.37 (1H, dqa, J=17.0, 1.5 Hz, $H16_{trans}$), 5.21 (1H, br d, J=10.5 Hz, $H16_{cis}$), 4.68 (2H, br d, J=5.4 Hz, H14), 4.10 (1H, br d, J=14.2 Hz, $H4_{eq}$), 3.58 (1H, t, J=13.5 Hz, $H4_{ax}$), 3.26 (1H, dt, J=14.4, 4.9 Hz, $H6_{eq}$), 2.95 (1H, dt, J=14.4, 9.3 Hz, $H6_{ax}$), 1.91 (1H, br qa, J=13.2 Hz, $H5_{ax}$), 1.67 (3H, s, H13), 1.50 (1H, dt, J=15.0, 3.4 Hz, $H5_{eq}$); ^{13}C NMR (DMSO-d_6) δ 173.0 (C8), 160.7 (C2), 140.0 (C12b), 139.1 (C8a), 134.1 (C15), 130.5 (C12), 130.3 (C11), 129.7 (C10), 128.5 (C12a), 126.3 (C9), 117.5 (C16), 102.6 (C1), 69.6 (C14), 50.6 (C4), 44.2 (C6), 31.4 (C5), 6.6 (C13); ^{15}N NMR (DMSO-d_6) δ 262 (N3), 182 (N3a), 121 (N7). Anal. Calcd for $C_{17}H_{19}N_3O_2$ (297.35): C, 68.67; H, 6.44; N, 14.13. Found: C, 68.60; H, 6.58; N, 14.09%.

*4.10.2. (Z)-2-Allyloxy-1-methyl-7-[(E)-propen-1-yl]-4,5,6,7-tetrahydropyrazolo[1,5-e]benzo[g][1,5]diazonin-8-one (**13b**)*

Yield: pale yellow microcrystals, 0.061 g, 18%; mp 139–141 °C; ν_{max} 1690, 1592, 1541, 1205, 1163, 779, 640 cm^{-1}; ^1H NMR ($CDCl_3$) δ 7.51 (1H, td, J=7.7, 1.7 Hz, H10), 7.47 (1H, td, J=7.7, 1.7 Hz, H11), 7.41 (1H, dd, J=7.6, 1.7 Hz, H9), 7.31 (1H, br d, J=7.5 Hz, H12), 6.91 (1H, br d, J=14.7 Hz, H19), 6.04 (1H, ddt, J=17.4, 10.4, 5.4 Hz, H15), 5.34 (1H, dqa, J=17.4, 1.7 Hz, $H16_{trans}$), 5.21 (1H, dqa, J=10.5, 1.7 Hz, $H16_{cis}$), 4.98 (1H, dqa, J=14.7, 6.3 Hz, H18), 4.69–4.63 (overlapping, m, 2H, H14), 4.08 (1H, br d, J=15.2 Hz, $H4_{eq}$), 3.60 (1H, t, J=13.8 Hz, $H4_{ax}$), 3.54 (1H, dd, J=14.9, 4.6 Hz, $H6_{eq}$), 3.32 (1H, dd, J=14.9, 9.8 Hz, $H6_{ax}$), 2.22 (1H, dqa, J=15.0, 10.0 Hz, $H5_{ax}$), 1.68 (overlapping, 6H, s, H13 and dd, J=6.3, 1.8 Hz, H17), 1.44 (1H, dt, J=15.0, 4.5 Hz, $H5_{eq}$); ^{13}C NMR ($CDCl_3$) δ 168.9 (C8), 161.0 (C2), 140.0 (C8a), 139.8 (C12b), 134.5 (C15), 130.0 (C12), 129.9 (C10), 129.7 (C11), 128.4 (C12a), 126.4 (C9), 125.7 (C19), 108.5 (C18), 102.6 (C1), 69.8 (C14), 50.3 (C4), 46.8 (C6), 26.8 (C5), 16.0 (C17), 6.5 (C13); ^{15}N NMR ($CDCl_3$) δ 261 (N3), 182 (N3a), 149 (N7). Anal. Calcd for $C_{20}H_{23}N_3O_2$ (337.42): C, 71.19; H, 6.87; N, 12.45. Found: C, 71.27; H, 6.96; N, 12.48%.

*4.10.3. (Z)-7-Allyl-1-methyl-3-[(E)-propen-1-yl]-4,5,6,7-tetrahydro-3H-pyrazolo[1,5-e]benzo[g][1,5]diazonin-3,8-dione (**14b**)*

Yield: white microcrystals, 0.037 g, 11%; mp 144–145 °C; ν_{max} 1662, 1651, 1565, 1483, 1215, 1177, 753, 648 cm^{-1}; ^1H NMR ($CDCl_3$) δ 7.59–7.50 (overlapping, m, 3H, H9–11), 7.39 (1H, br d, J=7.39 Hz, H12), 6.57 (1H, dqa, J=14.3, 1.7 Hz, H14), 5.79 (1H, m, H18), 5.64 (1H, dqa, J=14.4, 6.7 Hz, H15), 5.20 (1H, dqa, J=10.4, 1.7 Hz, $H17_{cis}$), 5.15 (1H, dqa, J=17.4, 1.7 Hz, $H17_{trans}$), 4.23 (1H, ddt, J=15.2, 5.3, 1.7 Hz, $H19_{exo}$), 3.84 (1H, br d, J=15.8 Hz, $H4_{eq}$), 3.58 (1H, ddt, J=15.2, 7.5, 1.7 Hz, $H19_{endo}$), 3.20–3.16 (overlapping, m, 2H, $H4_{ax}$ and $H6_{eq}$), 2.88 (1H, dd, J=15.4, 10.3 Hz, $H6_{ax}$), 1.84 (3H, dd, J=6.8, 1.7 Hz, H16), 1.72 (3H, s, H13), 1.62 (1H, br qa, J=14.9 Hz, $H5_{ax}$), 1.27 (1H, dt, J=15.0, 4.5 Hz, $H5_{eq}$); ^{13}C NMR δ 170.4 (C8), 166.4 (C2), 153.4 (C12b), 138.9 (C8a), 132.9 (C18), 130.8 (C10), 129.8 (C11), 129.6 (C12), 127.5 (two coalesced lines, C9 and C12a), 121.5 (C14), 118.3 (C17), 116.1 (C15), 112.2 (C1), 50.5 (C4), 48.6 (C6), 48.4 (C19), 24.3 (C5), 15.5 (C16), 7.8 (C13); ^{15}N NMR ($CDCl_3$) δ 153 (N3), 105 (N3a), 124 (N7). Anal. Calcd for $C_{20}H_{23}N_3O_2$ (337.42): C, 71.19; H, 6.87; N, 12.45. Found: C, 71.24; H, 6.97; N, 12.38%.

4.11. Bridging of 5b by dialkylation with 1,3-bis(bromo methyl)benzene: (*Z*)-1-methyl-2-*O*-7-(benzene-1,3-diyldi methanediyl)-4,5,6,7-tetrahydropyrazolo[1,5-*e*]benzo [*g*][1,5]diazonin-8-one (15b)

Under Ar atmosphere to the mixture of NaH (0.24 g, 10 mmol) and THF (80 mL), **5b** (2.57 g, 10 mmol) was added in small portions. The resulted yellowish suspension was stirred for ca. 5 min at 25 °C until the hydrogen evolution was stopped. 1,3-Bis(bromomethyl)benzene (2.64 g, 10 mmol) was added in one portion to this mixture, which was then refluxed for 30 min and cooled to 25 °C. After addition of the second portion of NaH (0.24 g, 10 mmol), the mixture was stirred at 25 °C for ca. 10 min, refluxed for 1 h and evaporated to dryness. The solid residue was dissolved in DCM (50 mL) and the undissolved salt was removed by filtration. The solution was extracted with water (2×50 mL), dried over $MgSO_4$ and evaporated. The resulted solid mixture was separated by flash column chromatography using *n*-hexane–EtOAc (5:1) as eluent. The first band visible on UV-irradiation was collected and evaporated. The white crystals of **15b** were washed with cold EtOH (5 mL), filtered off and dried. Analytical sample was recrystallized from EtOH. Yield: white cubic crystals, 0.970 g, 27%; mp 251–252 °C; ν_{max} 1639, 1480, 1419, 1196, 947, 760, 651 cm^{-1}; ^1H NMR ($CDCl_3$) δ 7.48 (1H, td, J=7.7, 1.8 Hz, H10), 7.43–7.39 (overlapping, m, 2H, H9 and H11), 7.30 (1H, br d, J=7.5 Hz, H17), 7.24 (1H, br d,

J=7.6 Hz, H12), 7.21 (1H, t, J=7.5 Hz, H16), 7.14 (br d, J=7.5 Hz, H15), 6.74 (1H, br s, H19), 5.61 (1H, d, J=14.3 Hz, H20$_{exo}$), 5.03 (1H, d, J=10.9 Hz, H13$_{exo}$), 4.88 (1H, d, J=10.9 Hz, H13$_{endo}$), 3.75 (1H, br d, J=14.5 Hz, H6$_{eq}$), 3.42–3.38 (overlapping, m, 2H, H4$_{ax}$ and H6$_{ax}$), 3.35 (1H, d, J=14.3 Hz, H20$_{endo}$), 3.28 (1H, dd, J=15.4, 5.3 Hz, H4$_{eq}$), 1.66 (3H, s, H20), 1.55 (1H, br qa, J=14.5 Hz, H5$_{ax}$), 1.30 (1H, dt, J=15.4, 4.5 Hz, H5$_{eq}$); ^{13}C NMR ($CDCl_3$) δ 170.7 (C8), 158.2 (C2), 140.6 (C8a), 140.1 (C12b), 139.4 (C18), 136.1 (C14), 132.1 (C19), 130.5 (two coalesced lines, C10 and C12), 129.6 (C17), 129.4 (C11), 128.8 (C15), 128.6 (C16), 128.0 (C12a), 108.9 (C1), 75.0 (C13), 53.7 (C4), 52.5 (C20), 50.0 (C6), 30.6 (C5), 7.0 (C21); ^{15}N NMR ($CDCl_3$) δ 282(N3),192(N3a), 135 (N7). Anal. Calcd for $C_{22}H_{21}N_3O_2$ (359.42): C, 73.52; H, 5.89; N, 11.69. Found: C, 73.54; H, 5.94; N, 11.74%.

Acknowledgements

The authors express their thanks to Dr. Medzihradszky-Schweiger for analyses.

Supplementary data

Supplementary data associated with this article can be found in the online version, at doi:10.1016/j.tet.2008.09.020.

References and notes

1. Reviews: (a) Nubbemeyer, U. *Top. Curr. Chem.* **2001**, *216*, 125; (b) Maier, M. E. *Angew. Chem., Int. Ed.* **2000**, *39*, 2073; (c) Evans, P. A.; Holmes, B. *Tetrahedron* **1991**, *47*, 9131 Selected examples: (d) Lindström, U. M.; Somfai, P. *Chem.—Eur. J.* **2001**, *7*, 94; (e) Bieräugel, H.; Jansen, T. P.; Shoemaker, H. E.; Hiemstra, H.; van Maarseveen, J. H. *Org. Lett.* **2002**, *4*, 2673; (f) Derrer, S.; Davies, J. E.; Holmes, A. B. *J. Chem. Soc., Perkin Trans. 1* **2000**, 2597.
2. (a) Aeberli, P.; Houlihan, W. J. *J. Org. Chem.* **1969**, *34*, 2715–2720; (b) Akitada, N.; Shoko, K. *Chem. Pharm. Bull. Tokyo* **1972**, *20*, 1445; *Chem. Abstr.* **1972**, *77*, 114378.
3. Bengelmans, R.; Herlem, D.; Husson, H.-P.; Khoung-Hun, F.; Le Goff, M.-T. *Tetrahedron Lett.* **1976**, *17*, 435–438.
4. Kurihara, T.; Sakamoto, Y.; Takai, M.; Ohishi, H.; Harusawa, S.; Yoneda, R. *Chem. Pharm. Bull.* **1995**, *43*, 1089–1095.
5. McDonald, I. M.; Dunstone, D. J.; Kalindjian, S. B.; Linney, I. D.; Low, C. M. R.; Pether, M. J.; Steel, K. I. M.; Tozer, M. J.; Vinter, J. G. *J. Med. Chem.* **2000**, *43*, 3518–3529.
6. Klapars, A.; Parris, S.; Anderson, K. W.; Buchwald, S. L. *J. Am. Chem. Soc.* **2004**, *126*, 3529–3533.
7. (a) Carniaux, J.-F.; Kan-Fan, C.; Royer, J.; Husson, H.-P. *Synlett* **1999**, 563–564; (b) Carniaux, J.-F.; Kan-Fan, C.; Royer, J.; Husson, H.-P. *Tetrahedron Lett.* **1997**, *38*, 2997–3000.
8. Simó, M.; Csámpai, A.; Harmat, V.; Barabás, O.; Magyarfalvi, G. *Tetrahedron* **2001**, *57*, 7191–7198.
9. Finner, F.; Zeugner, H.; Benson, W. *Arch. Pharm. (Weinheim)* **1989**, *322*, 507.
10. Aversa, M. C.; Giannetto, P.; Romeo, G.; Ficcara, P.; Vigorita, M. G. *Org. Magn. Reson.* **1981**, *15*, 394.
11. Gilman, N. W.; Rosen, P.; Earley, J. V.; Cooke, C. M.; Todaro, L. J. *J. Am. Chem. Soc.* **1990**, *112*, 3969.
12. Gilman, N. W.; Rosen, P.; Earley, J. V.; Cooke, C. M.; Blount, J. F.; Todaro, L. J. *J. Org. Chem.* **1993**, *58*, 3285.
13. Sanner, M. A.; Josef, K.; Johnson, R. E.; D'Ambra, T.; Kowalczyk, P.; Kullning, R. K.; Michaels, F. *J. Org. Chem.* **1993**, *58*, 6417.
14. Katritzky, A. R.; Fan, W.-Q.; Greenhill, J. V.; Steel, P. J. *J.Org. Chem.* **1991**, *56*, 1299.
15. Simeonov, M. F.; Fülöp, F.; Sillanpää, R.; Pihlaja, K. *J. Org. Chem.* **1997**, *62*, 5089–5095.
16. Andronati, S. A.; Rudenko, O. P.; Bogatskii, A. V. *Zh. Obshch. Khim.* **1975**, *45*, 389–396.
17. Andronati, S. A.; Chepelev, V. M.; Voronina, T. A. *Khim. Farm. Zh.* **1985**, *19*, 535–539.
18. Endo, Y.; Imada, T.; Yamaguchi, K.; Shudo, K. *Heterocycles* **1994**, *39*, 571–579.
19. Elguero, J.; Fruchier, A.; Llouquet, G.; Marzin, C. *Can. J. Chem.* **1976**, *54*, 1135–1138.
20. Kleinpeter, E.; Schroth, W. *Z. Chem.* **1989**, *29*, 62–63.
21. Miglia, O.; Lamartina, L.; Rainieri, R. *J. Heterocycl. Chem.* **1995**, *32*, 1589–1593.
22. Miglia, O.; Plescia, S.; Diana, P.; DiStefno, V.; Camarda, L.; Dall'Olio, R. *Arkivoc* **2004**, *5*, 44–53.
23. Kawai, T.; Endo, Y.; Shudo, K.; Itai, A.; Yamaguchi, K. *Acta Crystallogr.* **1993**, *B49*, 769–773.
24. Bremner, J. B.; Russell, H. F.; Shelton, B. V.; White, A. H. *Heterocycles* **2000**, *53*, 277–290.
25. Bremner, J. B.; Sengpracha, W. *Tetrahedron* **2005**, *61*, 941–953.
26. Broggini, G.; Garanti, L.; Molteni, G.; Zecchi, G. *Org. Prep. Proced. Int.* **1996**, *28*, 699–701.
27. Körmendy, K.; Ruff, F.; Kövesdi, I. *Acta Chim. Hung.* **1986**, *125*, 415–426.
28. Körmendy, K.; Kálmán, A.; Koritsánszky, T.; Kövesdi, I.; Sohár, P.; Ruff, F. *Acta Chim. Hung.* **1986**, *123*, 15.
29. (a) Parr, R. G.; Yang, W. *Density Functional Theory of Atoms and Molecules*; Oxford University Press: New York, NY, 1989; (b) Zeigler, T. *Chem. Rev.* **1991**, *91*, 651–667.
30. Becke, A. D. *J. Chem. Phys.* **1993**, *98*, 5648–5652; (b) Lee, C.; Yang, W.; Parr, R. G. *Phys. Rev. B* **1988**, *37*, 785–789.
31. Hehre, W. J.; Radom, L.; Schleyer, P. V. R.; Pople, J. A. *Ab initio Molecular Orbital Theory*; Wiley: New York, NY, 1986.
32. Miertus, S.; Scrocco, E.; Tomasi, J. *J. Chem. Phys.* **1981**, *55*, 117.
33. Szabó, A.; Csámpai, A.; Körmendy, K.; Böcskey, Zs. *Tetrahedron* **1997**, *53*, 7021–7034.
34. (a) Sutherland, I. O.; Ramsay, M. V. J. *Tetrahedron* **1965**, *21*, 3401; (b) Lansbury, P. T.; Saeva, F. D. *Tetrahedron Lett.* **1966**, *48*, 5991; (c) Kessler, H. *Angew. Chem.* **1970**, *82*, 237; (d) Dosen-Micovic, L.; Allinger, N. L. *Tetrahedron* **1978**, *34*, 3385; (e) Larive, C. K.; Rabenstein, D. L. *J. Am. Chem. Soc.* **1993**, *115*, 2833; (f) Soi, A.; Bauer, W.; Mauser, H.; Moll, C.; Hampel, F.; Hirsch, A. *J. Chem. Soc., Perkin Trans. 2* **1998**, *6*, 1471.
35. Schlegel, H. B. *J. Comput. Chem.* **1987**, *3*, 214.
36. (a) Peng, C.; Ayala, P. Y.; Schlegel, H. B.; Frisch, M. J. *J. Comput. Chem.* **1996**, *17*, 49; (b) Ayala, P. Y.; Schlegel, H. B. *J. Chem. Phys.* **1997**, *107*, 375.
37. Tapia, O.; Andrés, J. *Chem. Phys. Lett.* **1984**, *109*, 471–477.
38. (a) *Handbook of Metathesis*; Grubbs, R. H., Ed.; Wiley-VCH: Weinheim, Germany, 2003; Vols. 1–3; (b) Trnka, T. M.; Grubbs, R. H. *Acc. Chem. Res.* **2001**, *34*, 18; (c) Grubbs, R. H. *Tetrahedron* **2004**, *60*, 7117; (d) Fürstner, A. *Angew. Chem., Int. Ed.* **2000**, *39*, 3012; (e) Nicola, T.; Brenner, M.; Donsbach, K.; Kreye, P. *Org. Process Res. Dev.* **2005**, *9*, 513; (f) Vinokurov, N.; Michrowska, A.; Szmigielska, A.; Drzazga, Z.; Wójciuk, G.; Demchuk, O. M.; Grela, K.; Pietrusiewicz, K. M.; Butenschön, H. *Adv. Synth. Catal.* **2006**, *348*, 931; (g) Martin, W. H. C.; Blechbert, S. *Curr. Top. Med. Chem.* **2005**, *5*, 1521.
39. (a) Alcaide, B.; Almendros, P.; Alonso, J. M. *Chem.—A Eur. J* **2003**, *9*, 5793; (b) Alcaide, B.; Almendros, P.; Alonso, J. M. *Chem.—Eur. J* **2006**, *12*, 2874; (c) Panayides, E.-L.; Pathak, R.; De Koning, C. B.; Van Otterlo, W. A. L. *Eur. J. Org. Chem.* **2007**, *29*, 4953.
40. (a) Alcaide, B.; Almendros, P. *Chem.—Eur. J.* **2003**, *9*, 1259; (b) Schmidt, B. *Eur. J. Org. Chem.* **2004**, 1865; (c) Hong, S. H.; Sanders, D. P.; Lee, C. W.; Grubbs, R. H. *J. Am. Chem. Soc.* **2005**, *127*, 17160; (d) Courchay, F. C.; Sworen, J. C.; Ghiviriga, I.; Abboud, K. A.; Wagener, K. B. *Organometallics* **2006**, *25*, 6074.
41. Frisch, M. J.; Trucks, G. W.; Schlegel, H. B.; Scuseria, G. E.; Robb, M. A.; Cheeseman, J. R.; Montgomery, J. A.; Vreven, T., Jr.; Kudin, K. N.; Burant, J. C.; Millam, J. M.; Iyengar, S. S.; Tomasi, J.; Barone, V.; Mennucci, B.; Cossi, M.; Scalmani, G.; Rega, N.; Petersson, G. A.; Nakatsuji, H.; Hada, M.; Ehara, M.; Toyota, K.; Fukuda, R.; Hasegawa, J.; Ishida, M.; Nakajima, T.; Honda, Y.; Kitao, O.; Nakai, H.; Klene, M.; Li, X.; Knox, J. E.; Hratchian, H. P.; Cross, J. B.; Adamo, C.; Jaramillo, J.; Gomperts, R.; Stratmann, R. E.; Yazyev, O.; Austin, A. J.; Cammi, R.; Pomelli, C.; Ochterski, J. W.; Ayala, P. Y.; Morokuma, K.; Voth, G. A.; Salvador, P.; Dannenberg, J. J.; Zakrzewski, V. G.; Dapprich, S.; Daniels, A. D.; Strain, M. C.; Farkas, O.; Malick, D. K.; Rabuck, A. D.; Raghavachari, K.; Foresman, J. B.; Ortiz, J. V.; Cui, Q.; Baboul, A. G.; Clifford, S.; Cioslowski, J.; Stefanov, B. B.; Liu, G.; Liashenko, A.; Piskorz, P.; Komaromi, I.; Martin, R. L.; Fox, D. J.; Keith, T.; Al-Laham, M. A.; Peng, C. Y.; Nanayakkara, A.; Challacombe, M.; Gill, P. M. W.; Johnson, B.; Chen, W.; Wong, M. W.; Gonzales, C.; Pople, J. A. *GAUSSIAN 03, Revision A. 1*; Gaussian, Inc.: Pittsburgh, PA, 2003.
42. Sheldrick, G. M. *SHELXS97-Program for Crystal Structure Determination*; University of Göttingen: Germany, 1997.
43. Sheldrick, G. M. *SHELXL97-Program for the Refinement of Crystal Structures*; University of Göttingen: Germany, 1997.